IDENTIFICATION APTAMERS SPECIFIC FOR CARCINOEMBRYONIC ANTIGEN AND IT'S ANALYTICAL APPLICATIONS

A Thesis
Submitted to the Graduate Faculty
of the
North Dakota State University
of Agriculture and Applied Science

By

Michelle Catherine Lund

In Partial Fulfillment of the Requirements
for the Degree of
MASTER OF SCIENCE

Major Department:
Chemistry

June 2017

Fargo, North Dakota

North Dakota State University
Graduate School

Title

IDENTIFICATION APTAMERS SPECIFIC FOR

CARCINOEMBRYONIC ANTIGEN AND IT'S ANALYTICAL

APPLICATIONS

By

Michelle Catherine Lund

The Supervisory Committee certifies that this ***disquisition*** complies with North Dakota State University's regulations and meets the accepted standards for the degree of

MASTER OF SCIENCE

SUPERVISORY COMMITTEE:

Dr. Goudong Liu
Chair

Dr. D.K. Srivastava

Dr. Zhongyu Yang

Dr. Xiwen Cai

Approved:

07-07-2017 — Date

Dr. Gregory Cook — Department Chair

ABSTRACT

Carcinoembryonic Antigen (CEA) is an approved cancer biomarker by the Food and Drug Administration (FDA) for the early detection, diagnosis, and for the use in the regular screening of patients at high risk for the development of cancer. Traditional methods to determine the concentrations of CEA are based on utilizing antibodies. In this project, a graphene oxide (GO)–assisted systematic evolution of ligands through exponential enrichment (SELEX) was used to identify DNA aptamers specific for CEA. The dissociation constants of the identified aptamers were determined with surface plasmon resonance (SPR). Comparison of the dissociation constants of aptamers isolated from the GO-based SELEX and affinity SELEX found the dissociation constant of the aptamers isolated from GO-assisted SELEX was three times lower than aptamers isolated from the affinity SELEX. The analytical applications of the identified aptamers were studied by developing a colorimetric test for the determination of CEA with un-modified gold nanoparticles.

ACKNOWLEDGEMENTS

This work would not have been possible without the help and support of Dr. Guodong Liu and his group; Sunitha Takalkar, Kwaku Baryeh and Xiaoguang Zhang who taught me much in the laboratory practices. I would also like to thank the visiting scholars who also gave some perspective to the work accomplished; Qiaobin Li and Yan Huang. I would also like to thank the Dr. Stuart Harring for allowing the use of some of his laboratory instruments and Dr. Estelle Leclerc for teaching me how to run surface plasmon resonance experiments and for the use of the two channel Reichert 2 SPR for without her help the comparison of the two SELEX methods would not have been possible. Finally, I would like to thank the National Institute of Health's Centers for Biomedical Research Excellence for which provided the funding for this research and it therefor would not be possible without this support.

TABLE OF CONTENTS

LIST OF TABLES

LIST OF FIGURES

LIST OF SCHEMES

LIST OF ABBREVIATIONS

CEA ……..... Carcinoembryonic antigen

SELEX …….. Systematic evolution of ligands through exponential enrichment

GO …….. Graphene oxide

FDA……. Food and Drug Administration

CA 125 ……..... cancer antigen 125

ELISA ……... enzyme-linked immunosorbent assay

RNA …….. Ribonucleic acid

DNA ……. Deoxyribonucleic acid

ssDNA ……..... Single stranded deoxyribonucleic acid

PEG …….. Polyethylene glycol

AMD ……..... age-related macular degeneration

IgE ……. immunoglobin E

SLE ……..... Systematic Lupus Erythaematosus

PDGF-r ……..... platelet derived growth factor receptor

CTLA -4 ……..... cytotoxic T-lymphocyte-associated protein 4

PSMA …….. Prostate specific membrane antigen

POC …… Point of Care

Con-A …….. concanavalin

AuNPs …… Gold nanoparticles

Tris HCl ……. …….. Trizma hydrochloride

PCR …… polymerase chain reaction

TCEP ……..... tris(2-carboxyethyl)phosphine

CE …… Capillary electrophoresis

SPR ……..... surface plasmon resonance

NexGen Sequencing ……. next generation sequencing

ITC ……..... isothermal calorimetry

EMSA……..... electrophoretic mobility shift assay

HEPES……..... 4-(2-hydroxyethyl)-1-piperazineethanesulfonic acid

TWEEN ……. Polyoxyethylene Sorbitan Monolaurate

BSA ……... Bovine Serum Albumin

$HAuCl_4$……..... Gold (III) chloride trihydrate

PBS …….. phosphate bufferered saline

PBS(T)……...……phosphate buffered saline with tween

SSC…….. Saline sodium citrate

RSD…… relative standard deviation

CA 19-9……...……carbohydrate antigen 19-9

IgG…….. Immunoglobulin G

LOD……..... limit of detection

NaCl…… Sodium chloride

$MgCl_2$……..... magnesium chloride

KCl……. ……Potassium chloride

$CaCl_2$…….. calcium chloride

CA 19-9 …….. carbohydrate antigen 19-9

CFB ……..... complementary factor B

LIST OF SYMBOLS

K_d……..……dissociation constant

M…….. molar

k ……. kilo

Da …… Daltons

L …….. Liters

C ……..... Celsius

nM ……..... nanomolar

µM ……. micromolar

µL ……. microliter

mL …….. milliliter

ng …… nanograms

picomolar ……. picomolar

nm …… nanometer

kcal ……..... kilo calories

mol …….. moles

cm …….. centimeters

s ……..... standard deviation

m …….. slope

CHAPTER 1. INTRODUCTION

This chapter introduces many aspects of this research. Topics to be covered in this chapter include: carcinoembryonic antigen (CEA) as a protein and its uses as a biomarker combined with its application in therapeutics and diagnostics as well as CEA detection methods and how these methods can be improved. The possibility of improvement in reported method will be through the use of aptamers and the process by which these aptamers are designed is with SELEX. CEA aptamers have already been reported using an affinity SELEX, however, other SELEX methods have not been well studied. Therefor in this study two types of SELEX methods will be analyzed using CEA as a target molecule since it has also very widely used protein biomarkers.

1.1. Background of Carcinoembryonic Antigen

Carcinoembryonic antigen, or more commonly known as CEA, is a glycoprotein that was first reported in 1965 by Gold and Freedman[1]. It was originally hypothesized that CEA was an oncofetal antigen, meaning that it is expressed specifically during fetal development while absent in healthy adults. CEA was then only re-expressed in the presence of cancers. However, this proved to be incorrect as it was then found to be expressed in healthy adult tissue[2]. This discovery opened up the possibility for CEA to become a potential biomarker.

The fact that CEA becomes elevated in the presence of cancer led to many studies being conducted on its gene family and structure. There have been 29 different genes/pseudogenes identified in the human CEA gene family. After further analysis, these genes were classified into three subgroups, the CEA subgroup, the PSG subgroup and a third subgroup[3]. CEA belongs to the immunoglobulin superfamily with two types of immunoglobin domains detected: the N-terminal domain and the Ig variable domain[4]. It was determined that CEA bulk production takes

place in the colon, and was therefore hypothesized that CEA could be a viable biomarker for colorectal cancer. This lead to many studies have being conducted to evaluate the strengths and weaknesses of CEA as a biomarkers.

1.2. Carcinoembryonic Antigen as a Biomarker

CEA was first accepted in 1974 by the Food and Drug Administration (FDA) for the early detection of cancer, diagnosis of cancer and for the use in the regular screening of patients at high risk for the development of cancer[5]. However, additional studies have found that CEA levels become elevated in not only colorectal cancer, but also in liver, lung, stomach, pancreatic, and ovarian cancer[6]. Meaning, CEA has a very poor sensitivity toward colorectal cancer. Even though CEA does not show any specificity toward colorectal cancer, at least for early detection, it still has many uses. The most important use of CEA is utilized in the prognosis, monitoring and assessment of the follow-up treatment in colorectal cancer. It can also be useful in the monitoring ovarian cancer when CA 125 is not elevated[7]. Another use of CEA is as a predictive marker for the risk of recurrence and risk of death measured over time for lung cancer[8]. Regardless of not being selective toward colorectal cancer, CEA is one of the most extensively used clinical tumor markers. This could be for several reasons, such as: CEA is a stable molecule, has a restricted expression in normal adult tissues and is typically expressed at high levels in positive tumors[9]. Because of CEA's versatility in monitoring certain diseases, it is not surprising it has been implemented in many analytical techniques and is of utmost importance in the implemented biosensors.

Even though it has been proven that CEA offers poor sensitivity toward specific cancers, this does not rule out its usefulness in monitoring many diseases. There is also the possibility that CEA, in combination with other proteins, could offer a more selective prognosis panel for early

detection of cancer, but CEA should not be used independently. With this possibility, it vital that a CEA detection methods be explored.

1.3. Introduction to Biosensors

There has been much interest in biosensor research and development over the last fifty years, since the first medical biosensor was reported by Professor Clark at the New York academy of Science in 1962 by Professor Clark[10]. Biosensors have a wide application in the medical field for the detection of pathogens, genetic disorders and cancers. The medical biosensors developed, hope to improve the sensitivity and selectivity of assays, while maintaining the reliability of the test. An important implication of this type of test is to hopefully reduce the time required for execution as well as result analysis. The main goal of such medical biosensors is to create a home based preliminary screening for a wide range of diseases.

There are two main elements of a biosensor. The first is a form of a bio-recognition element that allows for the interaction of the target substance which then produces a readable signal. Without the bio-recognition element, there would be no readable signal output. Therefore, it is of the utmost importance that this bio-recognition element be selective toward the target to produce a specific test. The second main element is a transducer. There have been many reported transduces that produce results in optical, electrochemical and piezoelectric output signals. When a biosensor is in its most basic form, it utilizes a form of bio-recognition element that is oable to interact stringently and selectively with a target substance or molecule, after which the binding event is transduced to provide readable signal. As stated above, the goal of such medical biosensors is to make available simple to use, home based testing, which is why there have been many method for the detection of carcinoembryonic antigen.

1.4. Detection Methods of Carcinoembryonic Antigen

Currently, the most reliable test for the measurement of CEA concentration in biological samples is with an ELISA test or an enzyme-linked immunosorbent assay. This type of method is often considered the gold standard in analytical chemistry and when testing a new method, it is not uncommon for the new method to be compared to an ELISA. In a typical sandwich assay of an ELISA, two antibodies are implemented. The first antibody, or capture antibody, is coated onto the surface of a well plate. When a target protein is present, it will bind with the capture antibody, while a secondary antibody will bind with the already bound protein, thus making a sandwich. On the secondary antibody, there is typically an enzyme present, that upon addition of a substrate, will induce a color change. This method is very useful since the darker the color change is, the higher the concentration of protein present, meaning the color is directly proportional to the amount of protein present in the solution. Other methods have been explored with the implementation of antibodies to detect CEA present in the solution. Some antibodies have been implemented in many analytical techniques such as electrochemical,[11,12, 13] fluorescent,[14] chemiluminescent,[15] label-free,[16] and even colorimetric[17]. Even though there have been many successful implementations of antibodies for the detection of CEA, there are many drawbacks when using antibodies such as expensive to produce, each batch that is produced can provide some variations, difficult to upscale for large production purposes, unstable at various temperatures and pH thus making it difficult to modify and finally they have a limited shelf life[18]. It is because of these drawbacks that many researches are looking for alternative ways to detect proteins, thus turning their attention toward aptamers.

1.5. Potential Improvements toward Reported Detection Methods

As stated before, there are many drawbacks when using antibodies, thus researches are now turning their attention toward aptamers. Aptamers are designed with SELEX or systematic evolution of ligands through exponential enrichment. Aptamers are single stranded RNA or DNA oligonucleotides and are fairly small in size and having a typical range from 20 to 60 nucleotides[18]. Aptamers got their name from the Latin "aptus" meaning to fit[19]. This could not be a more appropriate name since aptamer can bind, or "fit," to a large variety of targets including, but not limited to: simple inorganic molecules, complex proteins and even entire cells. It is because of this that aptamers are considered as nucleotide analogues of antibodies[20]. Not only do aptamers bind to a large range of targets, but an aptamer's binding ability is considered to be comparable to antibodies. This is measured through dissociation constants(K_d) which have been reported for aptamers in the low nano-molar to high pico-molar range[21]. However, aptamers have many advantages over antibodies. The first is that aptamers are much easier and cheaper to produce than antibodies,[20] because aptamers can be chemically synthesized. This process is well defined, highly reproducible, sequence independent, as well as can be easily up scaled for large production quantities, while the production of antibodies can require bacteria, cell cultures or animals, making the production of antibodies very time-consuming, and labor intensive[22]. Not only is the production of aptamers easier, aptamers are also neither immunogenic nor toxic[23]. Finally, the last advantage is that aptamers are smaller than antibodies, resulting in better tissue penetration and faster blood clearance than antibodies[24]. It is because of these reasons that aptamers are ideal candidates for early diagnostic as well as therapeutic purposes. It is therefor not surprising that many aptamers have already been implemented in the medical field.

1.6. Aptamers Implemented in Therapeutics and Diagnostics Purposes

There are many aptamers that have been implemented in therapeutics and diagnostics practices. For therapeutics aptamers have been implemented in many ways such as treatment of diseases, allergies, prevention of autoimmune disorders, and in the treatment of diabetes[25].

One of the first FDA-approved aptamer for therapeutic applications is called Macugan in which the modified nucleotides were used: F-2'-fluoronucleotide, m-2'-O-methylnucleotide followed by being conjugate to 40 kDa polyethylene glycol or PEG[26]. The large PEG that is conjugated onto the aptamer stops nucleases. Macugen was first approved by the FDA in 2004 and initially developed by NeXstar pharmaceuticals. Macugen as an aptamer that is used for the treatment of wet AMD or age-related macular degeneration, where macular degeneration is a disease that effects the eyes where there is an abundance of leaky blood vessels that can cause blindness in patients if the disease goes untreated. Macugen helps by binding to 165 isoform of vascular endothelial growth factor stopping the interactions with the receptors present on the blood vessels in the eyes, effectively stopping the excess growth of blood vessels, thus preventing blindness in the patient[27]. This is just one of the examples in how aptamers have been successfully implemented in the treatment of diseases. It can also be implemented in the help of treating allergic responses.

A DNA aptamer was designed by the Mendonsa group in 2004 which can mask the allergic response[28]. In order to understand how this works it is necessary to understand how an allergic response occurs. For type 1 allergens, immunoglobin E (IgE) is involved in type 1 hypersensitivity reaction. Type 1 allergens are mainly due to environmental factors such as grass, dust, pollens or food which then activates the immune system to over produce IgE antibodies. This overproduction can cause asthma, allergies and dermatitis. When the immune complex

binds to mast cell it can rupture the cell membrane releasing large amounts of granules which contains mediators such as histamine, serotonin, prostaglandins, and cytokines. These mediators are involved in smooth muscle contraction thus causing a hypertensive response[29]. This response can be stopped by the aptamer designed by Mendonsa which inhibits the interaction between the antibody and the mast cell, thus stopping the cascade effect. Not only are aptamers used in helping with the allergic responses but it has also been used to prevent autoimmune disorders such as Systemic Lupus Erythaematosus (SLE).

In the case of SLE is when auto-antibodies are generated against a persons own DNA, red blood cells and platelet membrane which can cause the lysis of the red blood cells leading to anemia as well as activate complement system that are involved in inflammatory responses and could cause tissue damage. Therefor, an RNA aptamer was selected to be against anti-DNA autoantibodies stopping the generation of antibodies[30]. This is just one example of how aptamers can be helpful in the treatment of autoimmune disorders. However, aptamers can also play a role in the treatment of diabetes.

An RNA aptamer has been designed to help treat diabetes as it has been designed to bind to a murine insulin receptor antibody –MA20. The MA20 antibody destroys the insulin receptors of murine which can cause diabetes[31]. When aptamer binds with MA20 it inhibits this process thus stopping the process of diabetes and thus stopping the damage of kidney. Another aptamer has known as NOX-E36 aptamer which targets chemokine CCL2, also stopping kidney damages[32]. These are just a few examples in which aptamers have been implemented in therapeutics, but aptamers have also been used for diagnostic purposes, such as for cancers.

Aptamers have been implemented for the diagnostics of cancer as well as the therapy for cancer treatment. There have been FDA approved aptamers for the following targets such as

PDGF-r, pigpen, CTLA-4, Tenascin-C, Siayl Lewis X, PMSA, and nucleolin, proteins as shown in the table below. Each target has been helpful in different cancers and just shows the wide variety of protein targets.

Table 1. FDA Approved Aptamers for Proteins in Cancer

Protein Target	Aptamer type	Role in Cancer
PDGF-r	DNA	Platelet Derived Growth Factor Receptor (PDGF-r) is a tyrosine kinase protein involves in metastasis of tumor (36)
Pigpen	DNA	Involved in blood vessel formation in cancer cells (37)
CTLA-4	DNA	Activated T cells further reduce the T cell response by raising threshold response needed for T-cell activation during cancer (38)
Tenascin-C	DNA	Activated during events such as fetal development, wound healing and in case of tumour growth (39-41)
Siayl Lewis X	DNA	Sialyl Lewis X is overexpressed in cancer cells and through selectin helps in metastasis process of cancer (42)
PSMA	DNA	PMSA has high expression and activity in prostate tumour can be used as possible biomarker as well as target site for cancer treatment (43-47)
Nucleolin	DNA	Recent studies have shown the presence of this protein on cell surface especially on cancer cells. (48,49)

As mentioned previously, there have already been aptamers identified toward CEA. Therefor the way in which these aptamers were identified will be discussed.

1.7. Aptamers Identified Toward Carcinoembryonic Antigen

There have been two published patents for the aptamers specific toward CEA. The first was published in 2010 and has thus far had its aptamer implemented in more analytical papers and therefor will be the main-focus of this study. However, the other sequences are listed in a table below. C.L. Smith identified the first aptamer sequence specific toward CEA[50] where the aptamer was designed using an already reported process by Ellington and Tuerk.[19, 51] Briefly, a

random sequence library comprised of a greater than 10^{14} different sequences with primers flanking either side of the random sequence. Initially the CEA was incubated with a random DNA library and then immobilized within a 500 μL Con-A column. The Con-A, also known as Concanavalin A which is a lectin and is able to bind to some sugar residues on some glycoproteins. Because of this, it is sometimes used to separate proteins that contain ceratin sugars from those that do not. The proteins containing the sugars can bind; whereas sugars that do not contain this will not bind. Once the proteins have been immobilized, the non-specific strands will be eluted. Since the specific strands will be in the column with the CEA protein. The non-specific strands are then discarded and then the CEA protein was then eluted. The proteins that bind to the concanavalin A can generally be eluted (detach) from the Con A by either changing the pH, the ionic strength, or by adding sugars that compete for the binding sites on the conA. In this case the CEA and aptamers were eluted with 0.5 M alpha-methyl-D-mannoside and 0.5 M alpha-methyl-D-glucoside dissolved in binding buffer. These sugars disrupt the interaction between the CEA and the immobilized ConA on the column. Once the CEA was eluted, the DNA strands were separated with the use of a phenol. The DNA strands were then amplified with a polymerase chain reaction or PCR creating a new DNA pool in which the selection process was repeated as shown in figure 1.

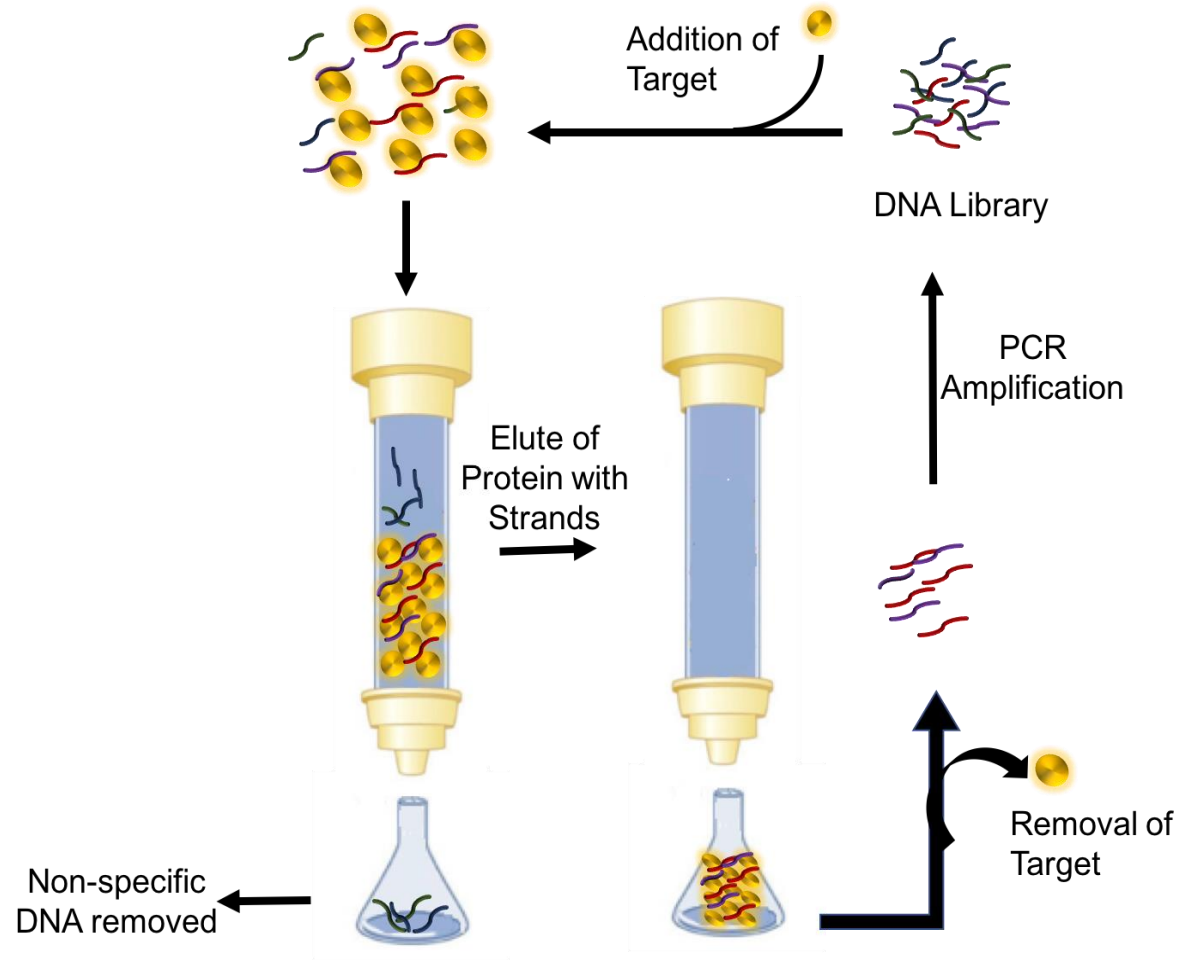

Figure 1. Affinity SELEX Method

For the identification of CEA aptamer this process was repeated 10 multiple times with positive and negative selection rounds were accomplished. After each round the library of aptamers that are specific toward CEA builds with a higher frequency of specific aptamers increases, as depicted in figure one.

As stated, two negative selection rounds were accomplished. This was done to reduce cross reactivity. The negative SELEX method is done in the following manner where the DNA library produced from the first five positive selection rounds were incubated with some counter targets. These targets can be proteins with similar structures or common proteins found in real samples. Then the counter targets were conjugated into the column, however the sequences that

would not be selective toward counter targets would be the first eliminated from the samples. These eluted sequences were then incubated with the target of choice and was carried on as if in a normal SELEX round. The counter selection in SELEX is very important since it can play a large roll in diminishing cross reactivity.

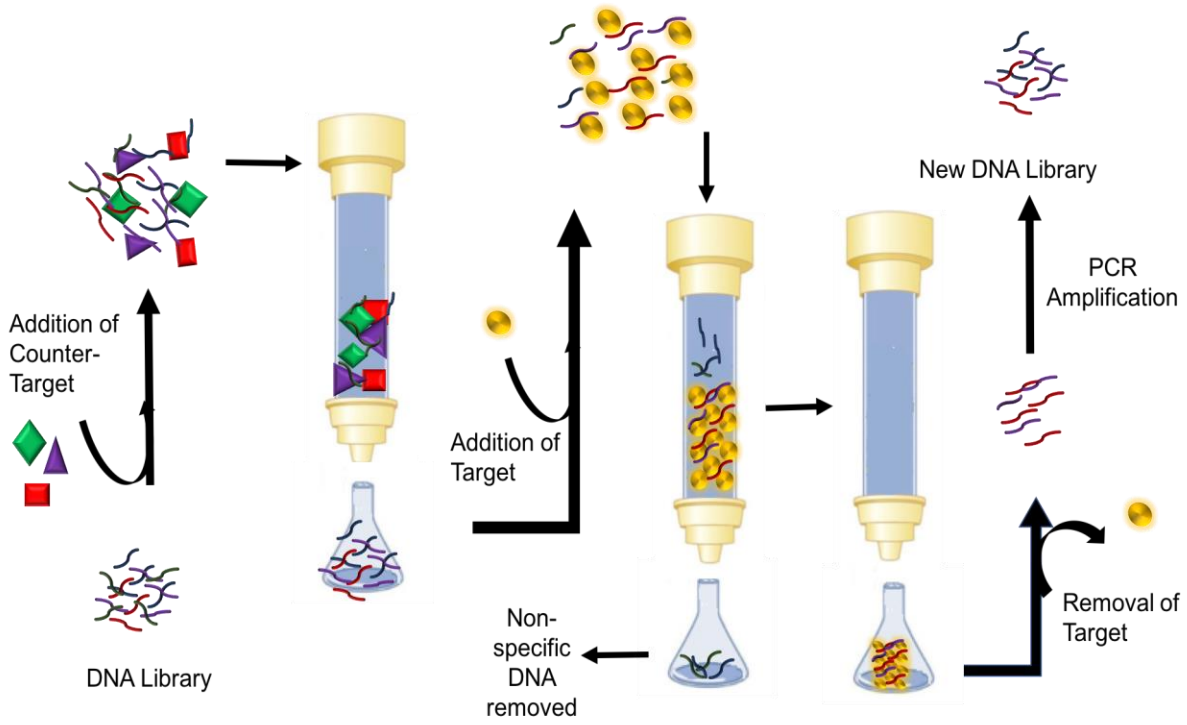

Figure 2. Negative Affinity SELEX Method

For the CEA aptamer, this negative counter selection was accomplished a total of two times. At the end of the SELEX method, the DNA pool that was produced was sent for sequencing eliminating an aptamer with the following sequence: 5' – ATA CCA GCT TAT TCA ATT – 3'

This aptamer has been implemented in many analytical techniques which will be discussed in the following sections.

Table 2. Reported CEA Aptamers

Sequence	Reported	Used in Analytical Techniques
5’ – TTT TTT TAT CCA AAG TTT TTT CGA ATA AGT – 3’ 5’- GCA GTT GAT CCT TTG GAT ACC CTG CTG – 3’		(52)
5’ – ATA CCA GCT TAT TCA ATT – 3’	(50)	(53-58)
5’- AAT TAA CCC TCA CTA AAG GGG AAT CCA ACT AAA CGT CCG – 3’ 5’ - ACC CTG CTA TAG TGT CAC CTA AAT CGT A – 3’ 5’ - GAC GAT AGC GGT GAC GGC ACA GAC GCC GCT ACC CCA TCC ACG CCA ATC CCG TAT GCC GCT TCC GTC CGT CGC TC – 3’ 5’ - GAC GAT AGC GGT GAC GGC ACA GAC GCC CCA GGA AGA ACC TAC TCA CTG ATC GTA TGC CGC TTC CGT CCG TCG CTC – 3’ 5’ - GAC GAT AGC GGT GAC GGC ACA GAC GTC CCG CAT CCT CCG CCG TGC CGA CCC GTA TGC CGC TTC CGT CCG TCG CTC – 3’ 5’- GAC GAT AGC GGT GAC GGC ACA GAC GCC CGC ATC CTC CGC CGT GCT GAC CCC GTA TGC CGC TTC CGT CCG TCG CTC – 3’ 5’ - GAC GAT AGC GGT GAC GGC ACA GAC GAA ATC CCC GCT GAA TTA CCA CTT TAC GTA TGC CGC TTC CGT CCG TCG CTC – 3’ 5’ - GAC GAT AGC GGT GAC GGC ACA GAC GCA CCG CTC TTA TGC CAC CAT TTT CAC GTA TGC CGC TTC CGT CCG TCG CTC – 3’ 5’ - GAC GAT AGC GGT GAC GGC ACA GAC GAA TTG GGA GTT AGT ATA CAT CTT ACC GTA TGC CGC TTC CGT CCG TCG CTC – 3’ 5’ - GAC GAT AGC GGT GAC GGC ACA GAC GAT AGG GAG CAT TAC GTA ACC ATC TCC GTA TGC CGC TTC CGT CCG TCG CTC – 3’ 5’ – GAC GAT AGC GGT GAC GGC ACA GAC GTG TTC AGG ATC GAG GGT ATT TCT GTG CGT ATG CCG CTT CCG TCC GTC GCT C – 3’	(59)	

1.8. Carcinoembryonic Antigen Aptamers Implicated in Analytical Techniques

As stated above, this aptamer has been implemented in many analytical techniques such as electrochemiluminescence,[55, 57] electrophoresis[53], fluorescence[58] and colorimetric[54]. The colorimetric assay is what we will focus on since any new aptamers developed in this experiment will be first developed for a colorimetric method.

In this method, unmodified gold nanoparticles (AuNPs) were used as a transducer to indicate if CEA was present. The first took a thiolated aptamer as reported above as:
5' – ATA CCA GCT TAT TCA ATT –SH - 3'

This aptamer was dissolved in 0.1 M phosphate-buffered saline(PBS) to make a 10 μM solution while 30 μL aptamer solution with 15 μL tris(2-carboxyethyl)phosphine (TCEP) was added to the samples containing different concentrations of CEA. It was then incubated for one hour at 37 ° C. This solution was then added to 500 μL of AuNPs and incubated for one hour. The salt was added to induce a color change from red to purple. If there is not protein present in the solution the AuNPs will remain red since the aptamers in the solution should interact with the gold surface thus keeping it stable. However if the CEA is protein is present, then the aptamers should interact with the CEA since it has a higher binding affinity toward that protein. Then the aptamers should leave the gold surface, destabilizing it and thus allowing for it to aggregate[54]. As is shown in the figure below.

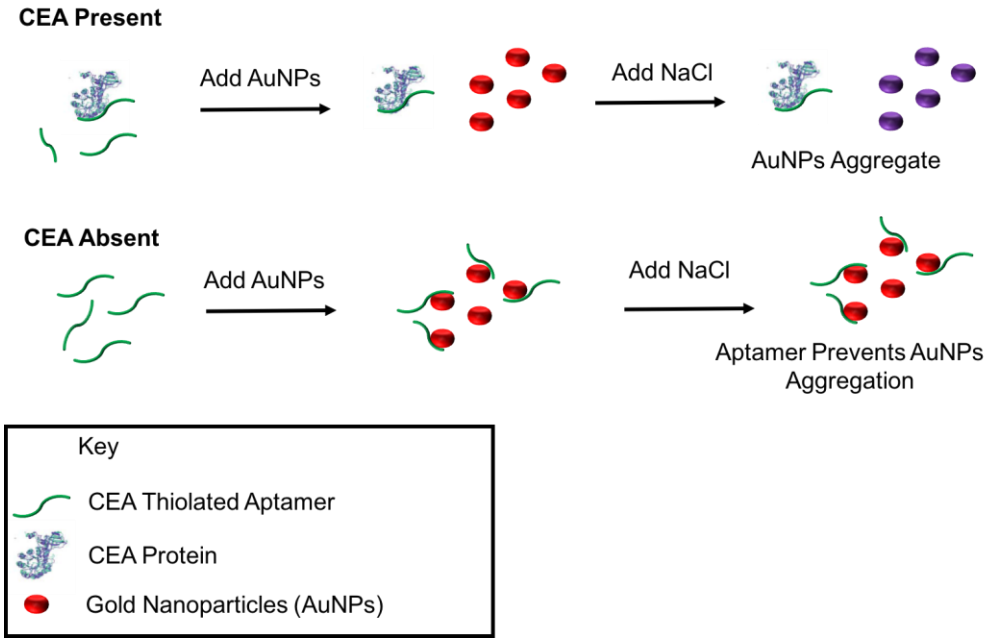

Figure 3. Colorimetric Method for the Detection of CEA Utilizing Specific Aptamer

In this method, there had been finite success for the detection of CEA with a limit of detection of 3 ng/mL. With a healthy cut off limit of 2.5 ng/mL, or 5 ng/mL, depending on the study being conducted this method provided a successful way in which CEA can be detected. This is an easy and simple colorimetric method that demonstrates that gold and be used to detect CEA in a solution with no modification. If an aptamer is designed with a new SELEX method an unmodified gold colorimetric method will be implemented.

1.9. Aims and Objectives of the Study

There are multiple aims for this study. The first is to determine which method of SELEX, the affinity column versus the graphene oxide assisted, as to which would more efficiently separate the specific and non-specific strands. The second main objective is to try to improve the reported detection methods of CEA with the implication of new aptamer.

1.10. Significance of the Study

There is a great significance to this study, since there have been great strides toward the identification of aptamers in hopes that they can replace or work alongside of aptamers, however there have not been any studies that have directly compared multiple SELEX methods. Therefore, it is of great importance that this is accomplished so a higher quality of aptamers can be designed. There is also a great significance for the second aim of this study. This is because no CEA aptamer has been implemented in a POC platform for success. If this is accomplished, this could have a great impact in the medical field, since it could potentially be used in a diagnostic manner, as well as monitoring the disease, increasing the quality of life for sick patients.

1.11. Limitations of the Study

There are a few limitations of this study. The first is that different personnel will be performing the two SELEX which means there could be some irregularities when performing the experimentation. Another is that the results from this experimentation will not be fully conclusive since this is the first study that has been accomplished. Therefor more experiments will have to be conducted.

CHAPTER 2. DEVELOPMENT OF CARCINOEMBRYONIC ANTIGEN APTAMERS UTILIZING GRAPHENE OXIDE ASSISTED SELEX

2.1. Literature Review of SELEX

Systematic evolution of ligands through exponential enrichment also known as SELEX, is used to identify aptamers. Aptamers, as introduced in the previous section, are classified as synthetically made, short single stranded sequences of DNA or RNA[60]. The SELEX process was first identified by two independent research groups. One group identified this process when designed RNA ligands to bind with bacteriophage T4 DNA polymerase[51] while another group designed RNA molecules that would bind specifically to certain ligands[19].

A positive outlook on SELEX is that it is not limited to a certain type of target. Aptamers have been identified for targets including proteins, heavy metals, bacteria and cells. Once aptamers have been identified, they are considered to be very specific and selective toward their intended target[61]. It is because of aptamers ability to bind specifically and selectively toward a certain target, that significant interest has been given toward aptamers and their design.

Since first described in 1990 many variations of the SELEX method have been made, some include using capillary electrophoresis (CE)[62], surface plasma resonance (SPR)[63] , mirco-free flow electrophoresis[64], as well as an automated method [65, 66] and even MonoLEX or a one-step aptamer protocol[67]. Some of these methods were described in the previous section showing how the SELEX process has been improved to limit the time and labor to complete this experiment.

Now, depending on the cost and the instrumentation available, this can place a limit on which method is used. There are many approaches to identifying aptamers, the one to be utilized in this study is known as graphene oxide assisted SELEX. This method is very like the similar to

the general outline of SELEX process where the starting random nucleotide library is incubated with the target, however to aid in the separation of bound strands from unbound strands, graphene oxide is added. The graphene oxide is added because it can effectively absorb DNA strands on its surface through π-π stacking[68]. After the separation is completed, the process continues as a typical SELEX method[44]. This is depicted below as graphene oxide- SELEX or GO-SELEX.

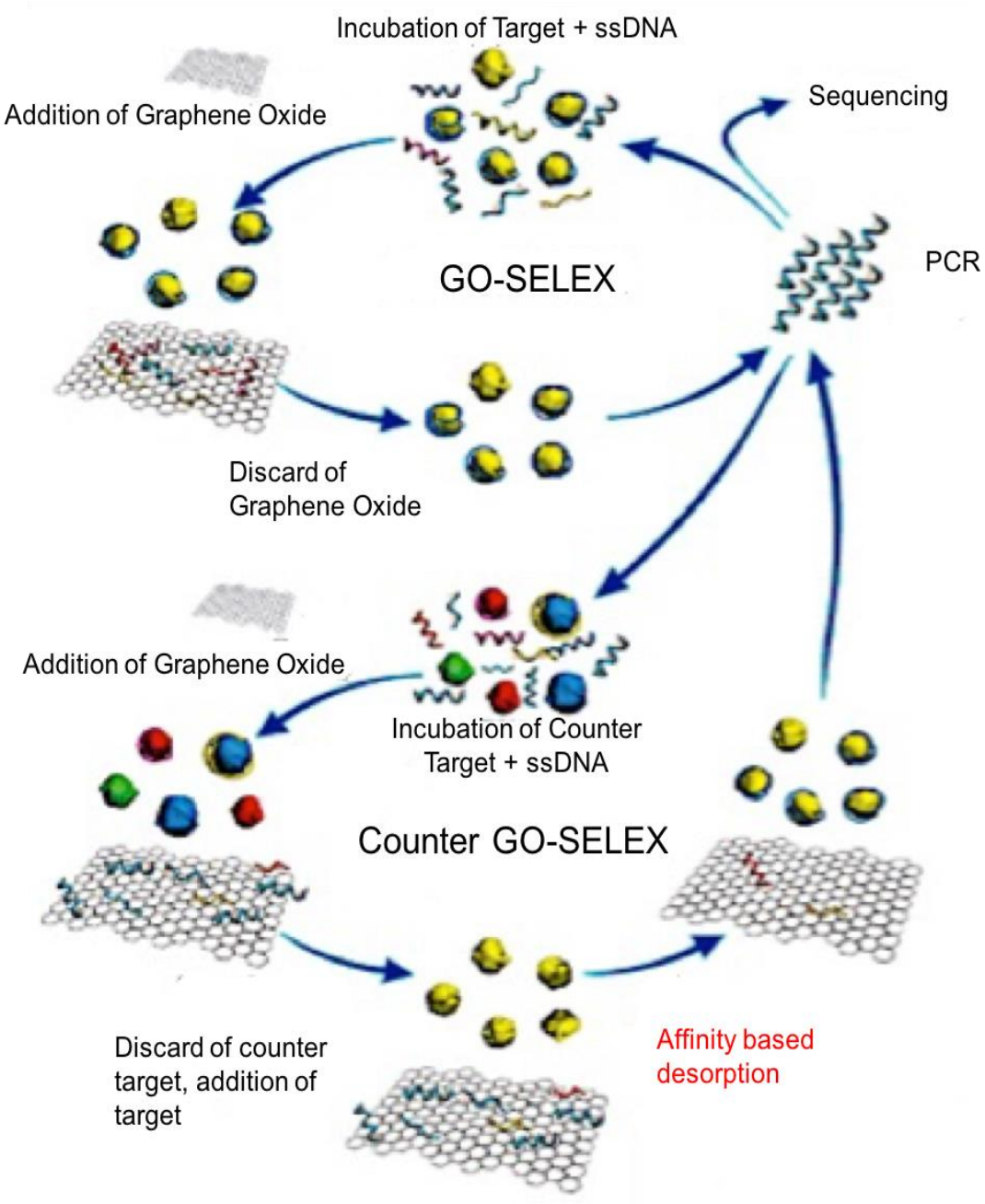

Figure 4. Graphene Oxide Assisted SELEX

As shown in the figure above, the method is based on, a counter selection round which is also shown. A counter selection round or negative selection round, is commonly used to ensure an even more selective and specific aptamer. This is done by using the DNA pool that has been generated from the positive selection rounds and incubated with targets that closely resemble the

target. This gives any strands that are specific toward the counter target, a chance to bind while the specific strands toward the target will stay in solution. By the addition of graphene oxide into the solution, the specific strands will interact and allow for the discard of the non-specific strands. Then the target is added into the solution containing both the graphene oxide and specific strands. These strands should have a higher binding affinity toward the target than toward the graphene oxide. Thus, the strands with a high specificity toward the target will leave the graphene oxide and bind to the target. The SELEX process then continues as a typical positive selection round. This counter selection is necessary so the aptamers that are developed have less cross reactivity, thus leading to a higher quality aptamer. In this experiment, both the positive and negative selection process will be implemented to design an aptamer. Once the aptamers have been designed, the most appropriate aptamer will have the most repeats after sequencing.

In this experiment, the two different types of SELEX will be compared while using CEA as a model protein. From here, it can be evaluated based on whether there have been improvements to the initial SELEX process as first described in 1990, as well as if the graphene oxide acts as a sufficient separation method.

2.2. Materials and Methods

2.2.1. Materials and Instrumentation for the Graphene Oxide SELEX Experiment

The following sources were used for purchase of materials used in this experiment were purchased from the following. The native carcinoembryonic antigen protein was purchased from Fitzgerald, while the trizma hydrochloride and phenol-chloroform-isoamyl solution was purchased from Sigma Aldrich. The primers and random nucleotide library were purchased from integrated DNA technologies and have the sequences as the following:

Random Library Sequence:

5'- ATC CAG AGT GAC GCA – NNN`30- TGG ACA CGGTGG CTT AGT - 3'

Forward Primer:

5' - Alex488N/ ATC CAG AGT GAC GCA GCA – 3'

Reverse Primer:

5' - BiosG/ ACT AAG CCA CCG TGT CCA – 3'

The dNTPs and Taq polymerase that were used for the polymerase chain reaction were purchased from New England Biolabs. The NAP- 5 columns, Sephadex G-25 DNA grade was acquired from GE Healthcare and the streptavidin agarose resin from Thermos Scientific. After each round of selection, the ssDNA the concentration was measured on a NanoDrop 2000c Spectrophotometer.

2.2.2. Graphene Oxide Assisted SELEX

The graphene oxide assisted SELEX was used to design aptamers for CEA. The aptamer was designed using a method that was previously reported[69]. Briefly for the positive SELEX round, 200 pmoles of a random nucleotide library were dissolved in 20 mM Tris HCl with a pH=7.4 and placed in a water bath of 95° C for five minutes, followed by an immediate placement in ice for fifteen minutes. Then, the ssDNA was incubated in equal concentration of CEA protein for one hour on ice with a gentle mix allowing for any specific strands to bind to the protein with the non-specific strands in the solution. Then graphene oxide was added to make a ratio of 1:8000, ssDNA to graphene oxide. This was incubated for another hour on ice with a gentle mix. The non-specific strands should then interact with the graphene oxide surface which can effectively absorb the DNA on its surface through π-π stacking[68]. This made it very easy to separate the specific strands from the non-specific strands. Upon this the sample was centrifuged

for fifteen minutes at 13 krpm in effectively separating the two, which allowed for the collection of the specific strands and the protein in the solution. To separate the protein from the bound DNA, an equal volume of phenol-chloroform-isoamyl was added. It was the shortly centrifuged to create two layers in which the top was collected containing the ssDNA. To conclude this round of selection, an ethanol precipitate was performed following a polymerase chain reaction to amplify the DNA. After the PCR the sample was double stranded but in order to start the next round the DNA must be converted into a single strand. This is why the reverse primer was tagged with a biotin. It was with this that when an affinity column is utilized, it causes the biotin to bind to the streptavidin which will then bind, thus when washed with sodium hydroxide, it will cleave the hydrogen bounds, thus washing out the forward strand, which can be used in the next round as is depicted is Scheme 1. After each round of selection, a nano-drop reading was taken to calculate the amount of DNA recovered after each round.

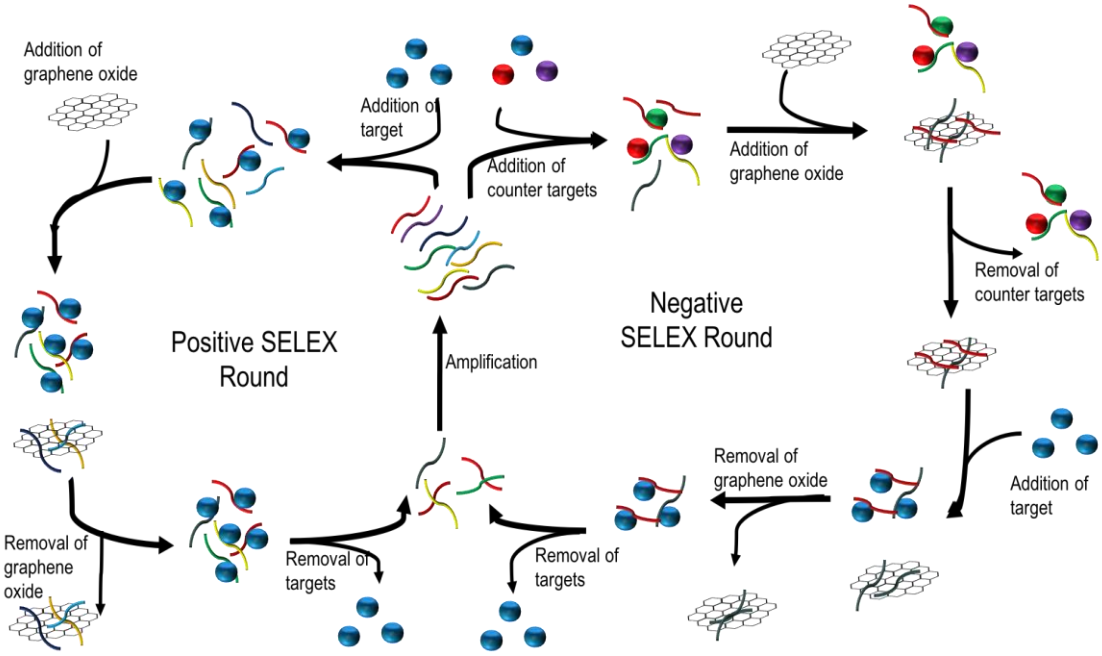

Scheme 1. Graphene Oxide Assisted SELEX showing Positive and Negative Selection Rounds

To reduce cross reactivity, there were multiple negative SELEX rounds accomplished. This process was repeated in a manner like that of the positive SELEX round in which 200 pmoles were incubated with protein of equal amounts. However, the protein in the negative selection round was carbohydrate antigen 19-9 (CA 19-9), bovine serum albumin (BSA), mammaglobin, and immunoglobulin G (IgG). This followed the positive selection round for when graphene oxide was added the strands specific toward CEA was interacted with the graphene oxide. The counter targets were then separated by centrifugation. The graphene oxide was then re-suspended in a solution containing 200 pmoles of the CEA, the DNA interacting with the graphene oxide would leave the surface and bind with the target protein since these strands should have a higher binding affinity toward the protein, in which the round continued as a positive SELEX round. This process is also depicted in Scheme 1. The total number of rounds performed of this was ten, accounting for seven positive rounds and three negative rounds. After the tenth round of selection the aptamers were then sent to the University of Florida for the Next Generation Sequencing given four potential aptamers. One of these aptamers where studied further to determine their dissociation constant with the use of surface of plasmon resonance (SPR), to be discussed in the following chapter.

2.3. Results

After each round of selection, a nano-drop reading was performed, and the percent of DNA recovered is shown in the following figures. In the figure 5, all rounds of selection were shown while in the sixth figure shows only the positive rounds of selection so that a trend can be accurately measured. In figure 5, the red boxes around the rounds, 6, 8 and 10 indicate that these were the negative selection rounds.

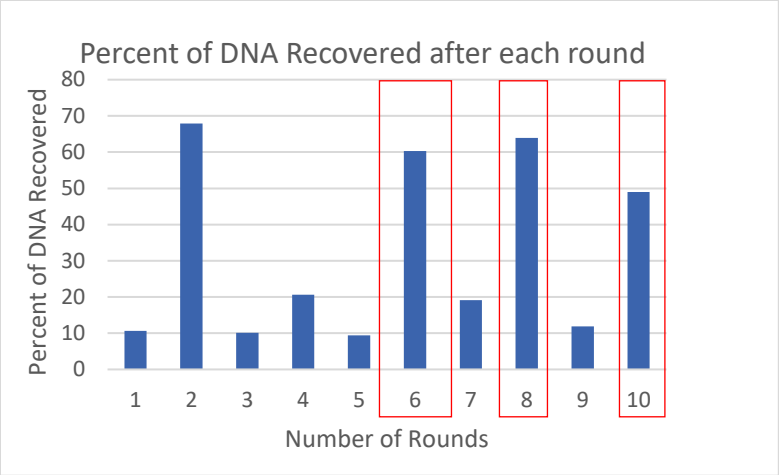

Figure 5. Percent of DNA Recovered from all Selection Rounds

While figure 6 just shows the percentage of DNA recovered from the positive selection rounds and is how it was determined to send the DNA pool for sequencing.

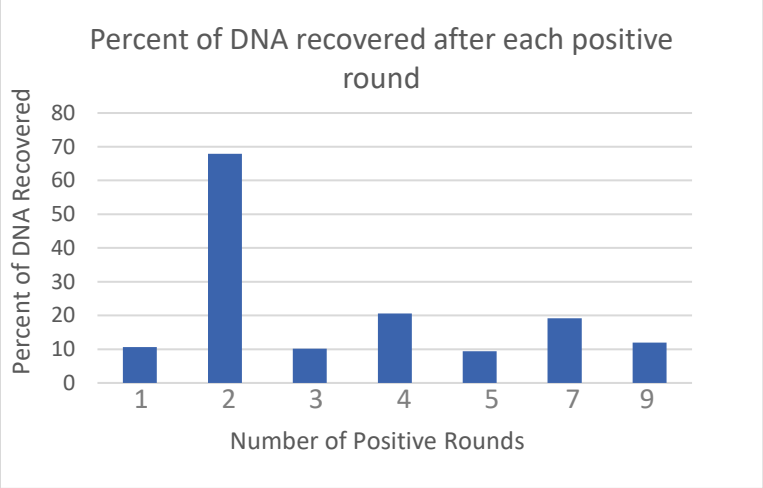

Figure 6. Percent of DNA recovered for all Positive Rounds

After the tenth round of selection with very little change in the percent of DNA recovered, the DNA pool was then sent to the University of Florida for sequencing using Next Generation Sequencing. From this, four potential aptamers were identified and provided in the table below.

Table 3. Aptamers Identified with GO-SELEX

	Sequence
CEA Apt 1	5’ – GGA ATC GGT GGC TTC ATG CTA GTC GCG GGC – 3’
CEA Apt 2	5’ – GCA GGG GTT TAA ATT GAC GAC TTA TCA CTG – 3’
CEA Apt 3	5’ – CCC TGC ACT ATC CTA TTC GAA TTG TTC CTG – 3’
CEA Apt 4	5’ – CGA AGT TAC GCT AGT CGG ATA CAA TTC TGGT – 3’

Aptamers one had the most repeating sequences and thus will only be studied further to determine the dissociation constant. Of these aptamers that have been isolated, none match the reported CEA aptamers from other papers.

2.4. Discussion

After each round of selection was accomplished, a nano-drop reading was done to evaluate the percent of DNA recovered. After round two, a sufficient amount of DNA was eliminated due to the graphene oxide separating the specific from the non-specific strands. Upon evaluating all rounds, it became apparent that the negative rounds of selection was not eliminating the DNA as efficiently as the positive selection rounds. Meaning, most of the DNA produced from the first five rounds of selection produced many DNA strands that were specific toward CEA. This is shown in figure five where the negative rounds are shown in the red boxes. As shown in figure six, there seemed to not be much change in the percent recovery from rounds seven to nine, even with a negative round in-between to indicate that most of the non-specific strands have been eliminated and that was ready for sequencing. Evaluating the results from the NextGen Sequencing, it became apparent that one of the four strands would be better suited for further investigation since the frequency in which aptamer 1 appeared is 7-10 times the amount of aptamers 3 and 4 and almost twice as often as aptamer 2. Therefor by accounting the number of repeated sequences, aptamer 1 is the only aptamer used in future experimentation.

2.5. Conclusion

In conclusion, based on the frequency of aptamers found by NexGen Sequencing, aptamer one is the only aptamer that will be further analyzed in future experiments and what will be used for the comparison for the GO-SELEX to the affinity SELEX, as that aptamer was mentioned in chapter one. This comparison of the two methods will be accomplished by finding the dissociation constant with surface plasmon resonance (SPR). This will be done in the following chapter.

CHAPTER 3. DETERMINATION OF DISSOCIATION CONSTANTS WITH SURFACE PLASMON RESONANCE

3.1. Literature Review of Methods for the Determination of Dissociation Constant

The dissociation constant is a specific type of equilibrium constant that measures the propensity of how a ligand can bind to a certain target and is the inverse of the association constant. This value is very important because it can quantify the quality of the aptamer and its ability to bind to its targets. Since this value is of great importance it is not surprising that many methods have been developed to determine this value. Some of these common methods would be; isothermal calorimetry(ITC), surface plasma resonance(SPR), electrophoretic mobility shift assay(EMSA), and fluorescent anisotropy. These methods will be explored, as well as the advantages and disadvantages discussed.

A common method is isothermal calorimetry or ITC. ITC experiments are performed using incremental titration where a precise volume of titrant is added to a solution of titrand at specific time intervals[70]. When the ligand binds to the target it releases or absorbs heat in direct proportion to the amount of binding that occurs[71]. This can produce a variety of peaks in which the area under each peak is integrated and then normalized to fit a model that allows for the calculation of affinity, enthalpy and the stoichiometry for the interaction[70]. There are many advantages to using ITC, the main is that it can provide a nearly complete thermodynamic characterization of an interacting system under one set of conditions[72]. These conditions being; standard state binding free energy (ΔG°), binding enthalpy (ΔH), and binding entropy (ΔS°) and are related by the equation below:

$$\Delta G^\circ = -RTlnK_{eq} = \Delta H - T\Delta S^\circ$$

Some other advantages is that it does not require immobilization and/or modification of protein or ligands since the absorption or production of heat is an intrinsic property of virtually all biochemical reactions[73]. The final advantage for this method is that this technique is relatively easy to perform[71]. However, there are some major draw backs to this method such as it can require a large amount of protein. This can mean that any concentration that is lower than high nano-molar is not sufficient to generate a significant injection heat signal and then the thermal gram is too shallow to be meaningful. This means that a high nano-molar sample concentration is chosen with a low pico-molar K_d binding system. This can lead to a steep titration curve with few points, thus giving rise to a large error in the dissociation constant[74]. This is just one of the methods that have been developed however another methods have been developed without the use of heavy instrumentation one of these methods is electrophoretic mobility shift assay.

The electrophoretic mobility shift assay, or EMSA, is done with the use of native gels because it can monitor the migration of DNA. When DNA becomes bound to a protein its molecular weight changes, thus slows the rate in which DNA migrates through the gel. When there is no protein bound, the DNA is fairly light in molecular weight, thus will travel the furthest through the gel, however, upon the binding of protein there will be a change in weight, and thus the DNA cannot travel as far as it had without the protein. From this, the dissociation constant can be determined from the amount of unbound and protein bound DNA in the gel[78].

This method is very popular because it is a highly sensitive, and low cost. However, this method has many drawbacks, the first is that it is very time consuming, taking 30 min to several hours depending on how long it takes to separate the bound from the unbound DNA. The other is that the dissociation is usually much slower than predicted based on solution measurements and distinct bands are obtained[74]. The final drawback of this method is that it typically uses a

radioactive label, thus making it dangerous to work with and can increase the cost of the experiment to discard the waste properly[79]. Even with these draw backs, EMSA is generally a more appropriate assay for the initial characterization of protein to ligand interaction, if binding is observed, experimental conditions can be optimized or another method can be used[80]. Another method that can be utilized is using fluorescence anisotropy intensity.

Fluorescence anisotropy is when there is light that is emitted by a fluorophore that will emit unequal intensities along the difference axes of polarization. When a ligand binds with protein or target present, there can be a change in fluorescence anisotropy. In most cases, the DNA is labeled with a fluorophore and the DNA will be emitting different light down different axes at a faster rate. Upon binding, the fluorophore starts rotating at a slower rate, thus increasing the fluorescence anisotropy. There are many advantages to using this method over the other methods mentioned. The first is that the use of fluorophores do not require special licensing and has no extra cost for the disposal of radioactive waste, unlike EMSA. The other is that these measurements only require a minuet amount of targets and oligonucleotides because the sensitivity of fluorescence, unlike ITC which requires a much larger amount of protein/target. The other is that this method does not require a step such as filtration or electrophoresis to separate the free or bound ligands. This may yield more true equilibrium binding constants[79]. This method, like most methods for determining the dissociation constant has a few disadvantages, some being that expensive equipment, is required using a fluorophore-labeled oligonucleotide is that the fluorophore label are typically large enough that they could potentially interfere with or otherwise influence binding. Therefor another method has been developed without the use of the fluorophore so this interference will not happen, an example of this method is the surface plasmon resonance.

Surface plasmon resonance (SPR) is special electromagnetic modes which may exist at the surface of a metal. The SPR works in the following manner, some polarized light will hit a metal film in which the interface of media will have a difference in refractive indexes. This will excite and detect the collective oscillations of free electrons, or surface plasmons, on the surface. This is accomplished with Kretschamnn configuration. This is where light is focused on the metal film through a glass prism and thus the reflection is detected. This change in refractive index can cause a dip in the reading and can be used for the determination of the dissociation constant by evaluating the shift in the reflectivity curve. This is done by monitoring the shift of the resonance vs. the time[75]. The advantages to using SPR, includes that it is a label free detection, the experiment can be accomplished within twenty minutes. The label free detection can help with the determining of both the thermodynamic and kinetic information[76]. However, whenever using this method caution should be employed. This is to ensure that the mass transfer of the protein from the bulk solution in the flow cell to the aptamers on the surface of the SPR. This can slow the observed association rate and give rise to an underestimation of the dissociation constant[77]. It is because of these drawbacks that in most cases it is necessary to perform binding studies with two different methods.

Speaking from a direct biochemistry background, the dissociation constant should be constant no matter what method is being implored. However, there can be many factors that will influence value, especially if the experimental conditions were not optimized such as: the type of buffer used for the experiment as well as the type of tag used on the aptamer, if the aptamer is free floating in solution and finally the sensitivity of the method could all lead to different dissociation constants being reported. This became clear in the reported aptamer. The reported aptamer had the dissociation constant calculated with two different methods. In method one they

choose to use EMSA and had a dissociation constant of 10^{-6} M, while the other method used was fluorescent anisotropy reading which found the dissociation constant to be ~ 10 nM[50]. It is therefore not uncommon to have two different dissociation constants reported when doing these studies and so when comparing the binding, the same method will have to be accomplished to ensure that a proper comparison can be accomplished. In this study, a surface plasmon resonance will be accomplished for the aptamer that was isolated in the graphene oxide assisted SELEX while the same method will be done on the reported aptamer. This study will help determine which aptamer binds more tightly toward the CEA target and thus allows for the quality of the aptamer to be determined.

3.2. Materials and Methods

3.2.1. Materials

The materials used in this experiment were purchased from the following companies: the HEPES, magnesium chloride, biotinylated BSA and TWEEN were all purchased from Sigma Aldrich. The streptavidin covalently immobilized on a carboxymethyl dextran surface gold chip in which all the experiments perform was obtained from Reichert and the CEA protein was purchased from Fitzgerald. The two biotinylated DNA was purchased from integrated DNA technologies which were aptamer one that was identified in the previous chapter and the aptamer that was identified in other works. Both aptamers have been modified with a biotin on the five-prime end and the sequences as follows:

Aptamer One:

5’ - /5Biosg/GGA ATC GGT GGC TTC ATG CTA GTC GCG GGC – 3’

Reported CEA Aptamer:

5’ - /5Biosg/ ATA CCA GCT TAT TCA ATT – 3’

All the experiments were performed on two channel Reichert 2 SPR and the data were analyzed using scrubber software, in which the dissociation constant was calculated.

3.2.2. Method of Conjugation

As stated above, the biotinylated aptamer was easily conjugated onto the surface of the gold chip. However, the method for the conjugation of the aptamers on the gold surface were different than how the dissociation constant was determined. The biotinylated aptamer was added under the following conditions: 250 μL injection of 50 nM biotin-aptamer followed by a five-minute dissociation and two wash cycles of 500 μL with a wait for one minute while keeping the infuse rate constant at 25 μL/min. This was done for both aptamer one isolated from chapter two and the reported aptamer in chapter one.

3.2.3. Dissociation Constant Titration and Determination

The way in which this experiment was conducted was done by the following scheme. Initially started with a gold chip that had streptavidin immobilized on a carboxymethyl dextran surface. Then there was 50 nM of biotinylated aptamer injected and would interact with the streptavidin on the gold surface. The addition of the biotinylated aptamer was only performed on the left channel since to the refractive index and peak intensity is found by taking the difference between the two channels. However, once the biotinylated aptamer was conjugated onto the gold surface, the following were done to both channels. Then 50 mg/mL of biotinylated BSA was added followed by a three hour incubation of BSA to block the excess streptavidin binding site to reduce non-specific binding for the CEA. The chip was then washed three times with running buffer containing 40 mM HEPES, 10 mM $MgCl_2$ and 0.005% TWEEN. This was to get rid of excess, non-bound BSA. Finally, different amounts of CEA was then added onto the chip. Since

CEA bound so quickly toward its aptamer it did not need a regeneration buffer, instead it was washed more with the running buffer. This is depicted below.

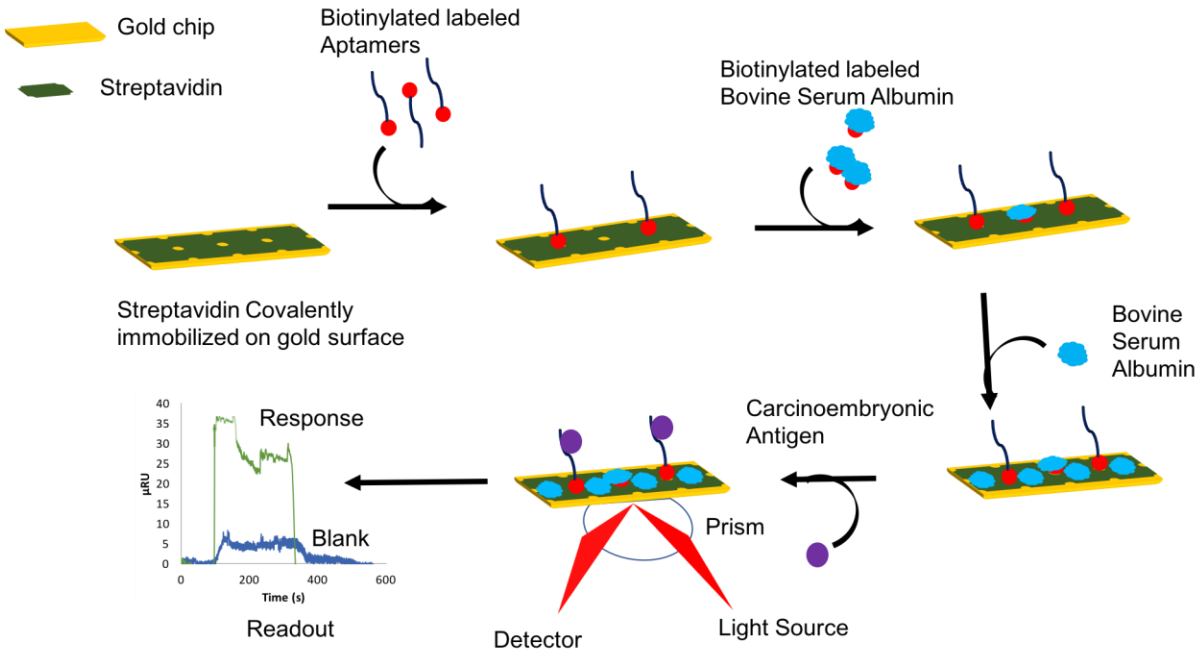

Scheme 2. Representation of Surface Plasmon Resonance Experiment

The parameters that were ran on the SPR for the measurement of the dissociation constant determination was programed as follows: 250 µL of the protein sample was injected over a span of four minutes followed by a five minute dissociation then the chip was regenerated with a 100 µL of running buffer for thirty seconds followed by a one minute dissociation. This was followed by two 500 µL wash cycles while the infuse rate was kept at a constant of 5 µL/min. This was kept constant for all samples taken. For aptamer one the concentrations evaluated were 75 nM, 125 nM, 250 nM, 750 nM and 1 uM of CEA and for the reported aptamer the concentrations measured were 750 nM, 1 µM, 2 µM and 3 µM.

3.3. Results

To ensure that the aptamer has indeed bound to the left side of the channel a certain trend must be observed as shown below. This was accomplished because of the binding between the biotin and streptavidin.

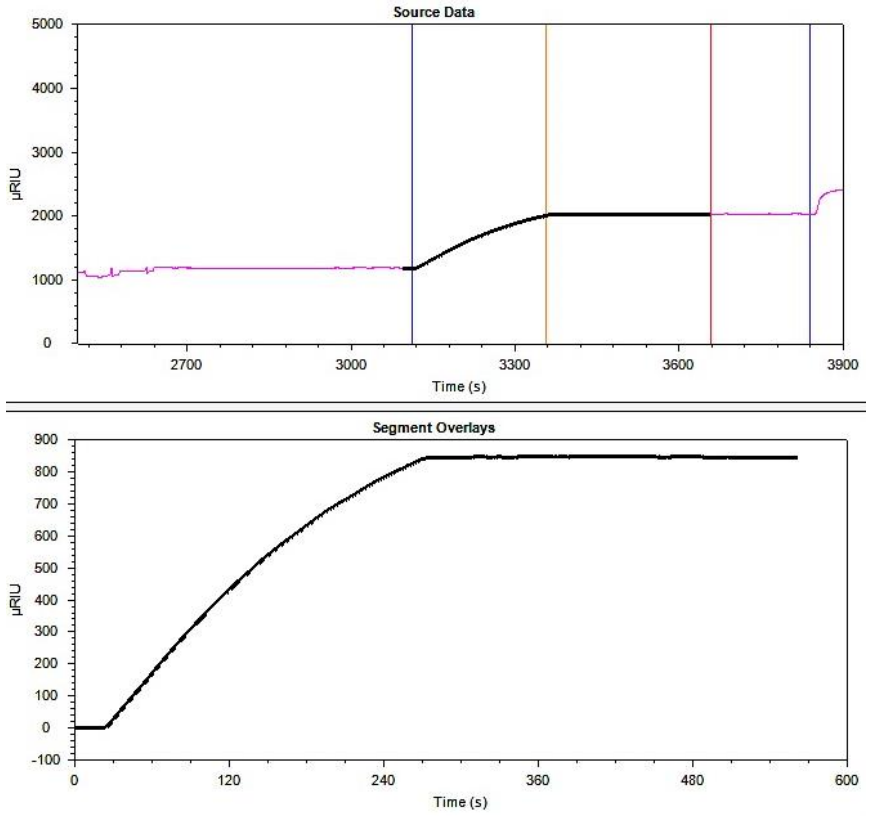

Figure 7. Proof of Conjugation of Aptamer onto the Gold Surface

The way in which the raw data was evaluated was performed on the Scrubber software. This was done by first zeroing out the initial peaks since that was caused by some background noise, it then was fitted with the curves. An example of this is shown in figure eight. This was accomplished for every experiment since it was done in triplicate for the aptamer that was isolated in the graphene oxide assisted SELEX method as well as for the reported aptamer from the affinity method.

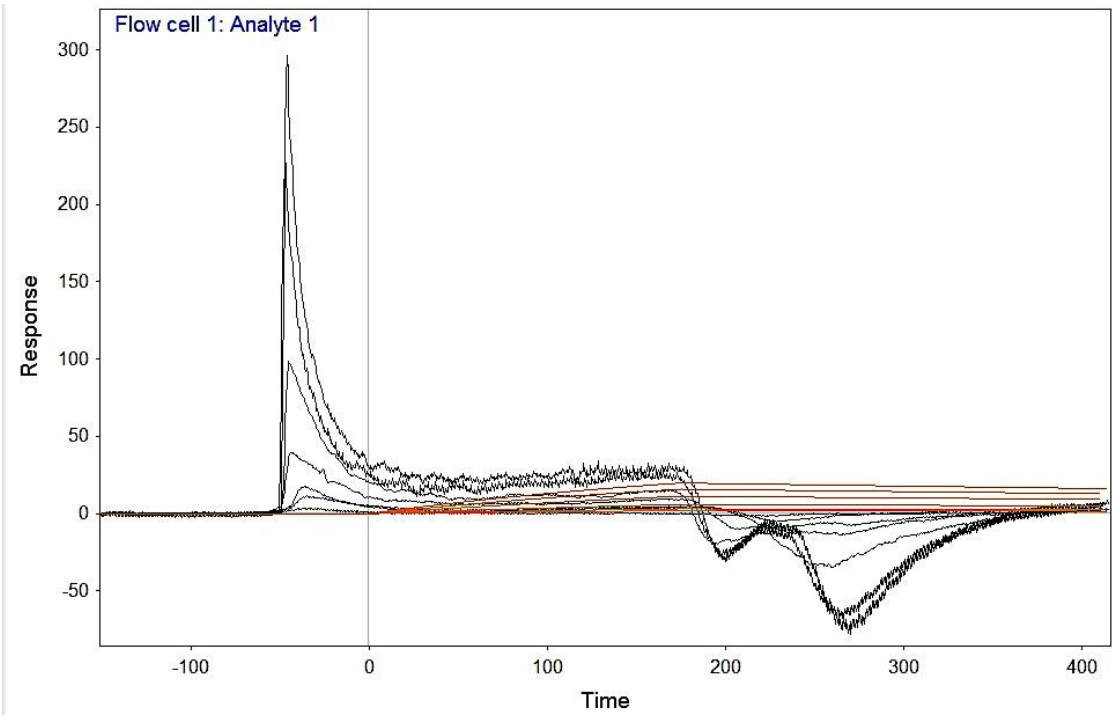

Figure 8. Aptamer One Curve Fitting in Scrubber Application of Raw Data for the Calculation of Dissociation Constant

These experiments were performed in triplicate in which the calculation of the dissociation constant was also accomplished three times. The average of this was done in the table below and had a dissociation constant calculated to be 253.68 ± 15.75 nM.

Table 4. SPR Determined Dissociation Constant for Aptamer One

Experiment	Dissociation Constant (nM)
1	235.64
2	260.17
3	264.68
Average	253.68
Standard Deviation	15.75

Another way to evaluate the data is to manually the plot the raw data and evaluate the peak intensity at a specific time. From this curve, a dissociation constant can be estimated. The

experiment was repeated three times with the concentrations of 75 nM, 125 nM, 250 nM, 750 nM and 1 uM of CEA. The peak intensities were then averaged and plotted to produce the graph below.

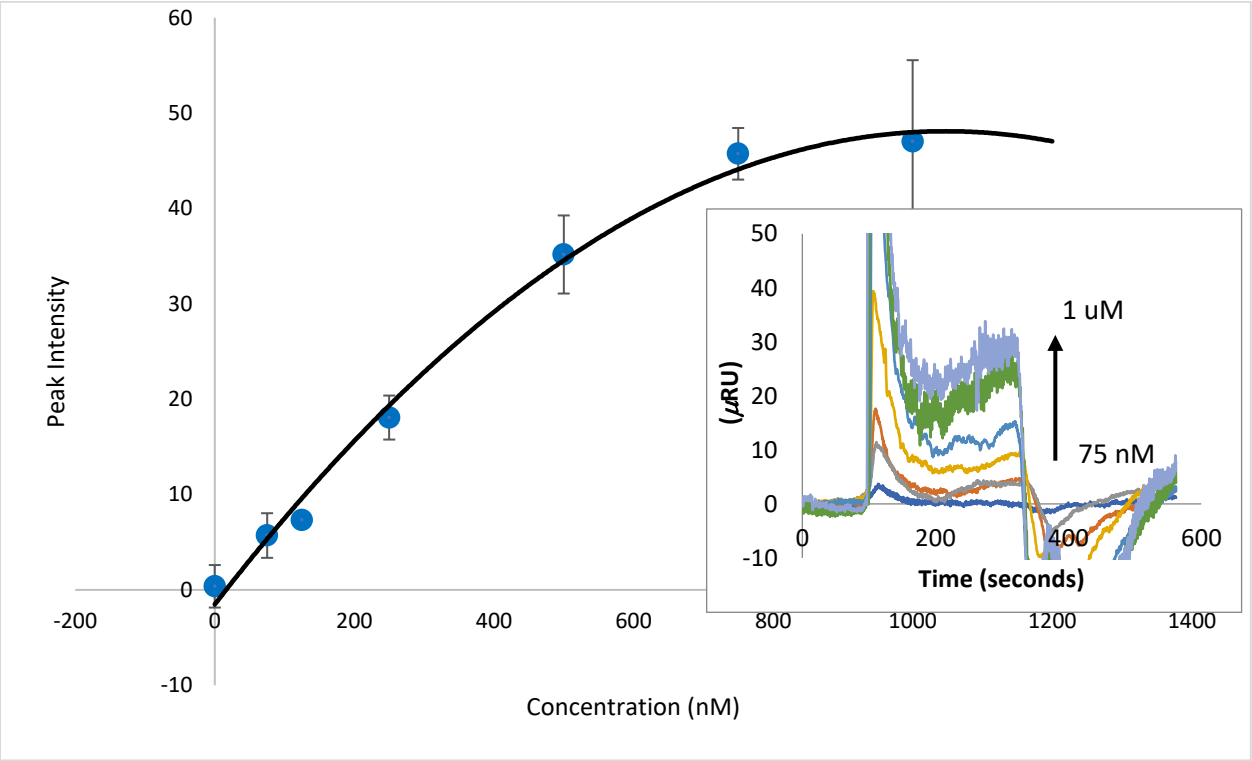

Figure 9. Curve fitting of the SPR Data to Calculate the Dissociation Constant for Aptamer One

After aptamer one was evaluated, the reported CEA aptamer was also accomplished in the same manner as aptamer one and also accomplished in the Scrubber software.

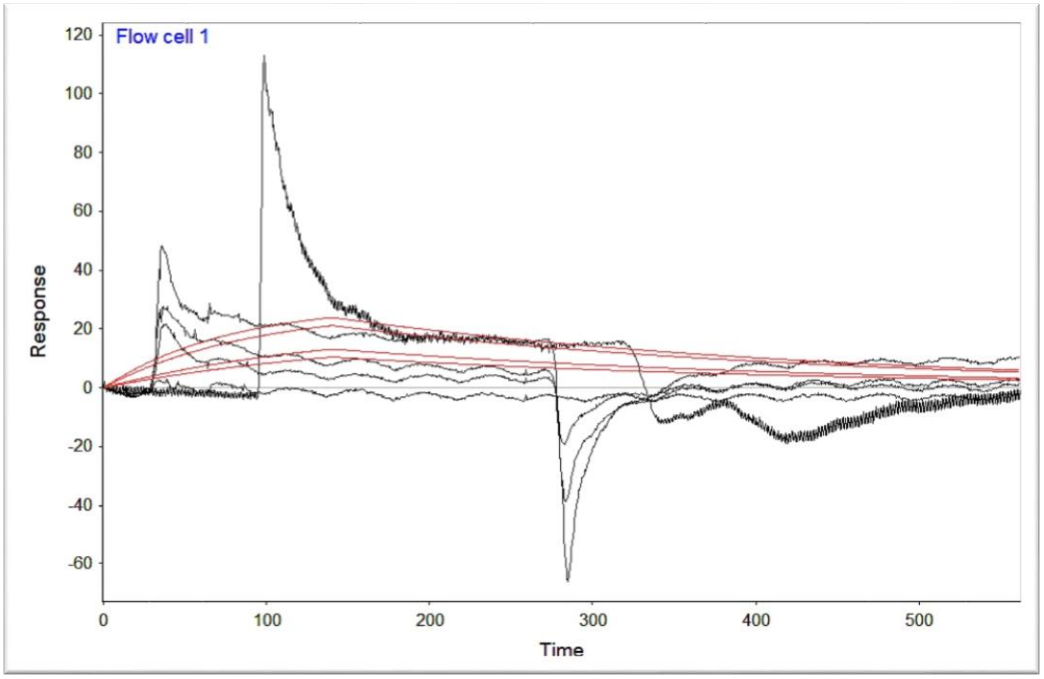

Figure 10. Reported Aptamer curve fitting in Scrubber application of Raw Data for the Calculation of Dissociation Constant

Based on the curve fitting, in the Scrubber application, three dissociation constants were calculated as shown in the table below in which these were averaged and had the standard deviation calculate. This allowed for the dissociation constant to be determined to be 828.26 ± 23.99 nM.

Table 5. SPR Determined Dissociation Constant for Reported Aptamer

Experiment	Dissociation Constant (nM)
1	831.57
2	850.43
3	802.79
Average	828.26
Standard Deviation	23.99

Not only was the data evaluated in the Scrubber application, the data was also examined in excel in which the data was plotted manually when the peak intensity was taken and plotted

against the concentration. In this case for the reported aptamer, there was no plateau until 2μM. The concentrations that were evaluated were 0.75, 1, 2, and 3 μM as shown in the figure below.

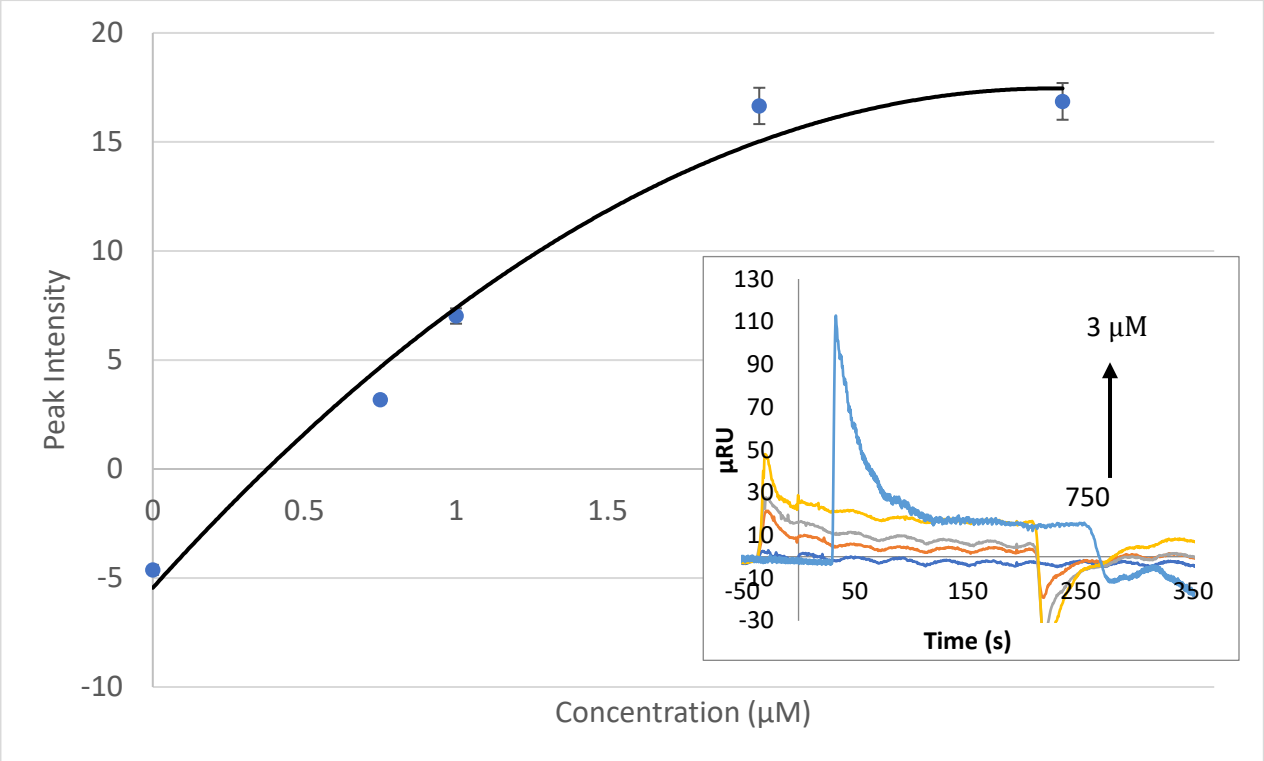

Figure 11. Curve Fitting of the SPR Data to Calculate the Dissociation Constant for Reported Aptamer

3.4. Discussion

This experiment first goal was to make sure that the aptamer identified in the previous chapter was indeed binding to carcinoembryonic antigen. The quality of the aptamer could be actively measured through the dissociation constant. For this experiment to be successful the aptamer need to be conjugated onto the gold surface therefor the first part of this experiment was to see that the aptamer was indeed binding to the gold chip surface. This was evaluated in figure seven. By seeing the large change in the response, and that the change was constant there

indicated that the biotin and streptavidin has bound and thus has successfully bound to the surface making the rest of the experiment possible.

Once the aptamer was conjugated on the gold surface the different concentrations of CEA were evaluated on the SPR, with an increasing concentration there was an increase in the response. The data was evaluated in two different ways. The first was on a software application called Scrubber in which the dissociation constant was calculated. The experiment was repeated three times giving three different dissociation constant values however the average of these were 253.68± 15.75 nM. This indicated that the CEA is binding to the aptamer fairly-tightly since aptamers have been reported to bind to their proteins from low micromolar to high picomolar range[74]. Another way in which the dissociation constant was estimated is by evaluating the michaelis-menten curve and taking half the V_{MAX} and seeing the K_M. The K_M is roughly 250 nM which corresponds to the calculated dissociation constant. It was confirmed that this dissociation constant was correct. This indicates that aptamer one is binding to CEA and thus is more likely to work in future biosensors.

Another goal of this experiment is to directly compare the aptamer that has been identified in the graphene oxide SELEX to the reported aptamer that has been identified in the affinity SELEX method. This was also accomplished in this study. A reported aptamer as also had a dissociation constant reported for it however, neither had a SPR done. The aptamer had a dissociation constant that was reported in the 10^{-6} M when used using electrophoretic mobility shift assay (EMSA) and in the low nanomolar range when using fluorescence anisotropy[50]. These each have some drawbacks since EMSA is not very sensitive while fluorescence anisotropy while being sensitive and being free floating in solution, the fluorescent tag can interact with a hydrophobic pocket thus providing a false dissociation constant. In this study, the reported

aptamer experiment was accomplished in the same manner as the aptamer identified in the previous chapter. However, more protein was needed to finish the titration and thus the aptamer had a dissociation constant that was calculated to be 828.26 ± 23.99 nM. This is significantly higher than the dissociation constant that was calculated in for aptamer one that was isolated in the graphene oxide assisted SELEX. This is an indication that aptamer one binds much more tightly to CEA than the reported aptamer. This value that was calculated for the reported aptamer was properly done by using the Scrubber application in which the data was fitted, along with the curve allowing for the calculation of this dissociation constant as shown in figure ten. This constant was also verified by plotting the raw data and taking the half of the V_{MAX} and visually seeing the K_M allowing for an estimation of the dissociation constant. By looking at the graph in figure 11, one could estimate the dissociation constant to be roughly 850 nM. This corresponds with the calculations that were completed indicating that this was done correctly. However, this value could be improved.

To confirm that the aptamer one is indeed better than the aptamer previously reported, another dissociation constant experiment could be accomplished with other methods mentioned previously such as ITC, EMSA or fluorescence anisotropy. There could also be improvements to the SPR experiment. This could be done by possibly by using a different gold chip surface in which the aptamer could be thiolated onto the gold surface and decrease the background noise thus lowering the dissociation constant. Another way is to by adding a 15 poly adenine to the five-prime end of the aptamers, thus increasing the distance between the gold surface and where the interaction takes place on the protein. This could allow for the aptamer to form its 3D configuration better and thus could possibly improve the dissociation constant.

3.5. Conclusion

In conclusion, this experiment was very successful in the determination of the dissociation constant for both the reported aptamer and the aptamer isolated in the previous chapter. The dissociation constant for the reported aptamer was found to be 828.26 ± 23.99 nM while the aptamer isolated with the graphene oxide assisted SELEX was found to be 253.68± 15.75 nM. This indicates that the aptamer isolated from the GO-SELEX binds more tightly to CEA than the aptamer isolated from the affinity-SELEX, thus graphene oxide can sufficiently separate the specific from the non-specific strands indicating that this GO-SELEX could be used for future experiments.

CHAPTER 4. UTILIZATION OF UNMODIFIED GOLD NANOPARTICLES FOR THE COLORIMETRIC DETECTION OF CARCINOEMBRYONIC ANTIGEN

4.1. Literature Review of Gold Nanoparticles

Gold nanoparticles or AuNPS are very common nanoparticles that are employed in aptasensors. The reason for this is that they offer many advantages such as ease of synthesis and surface modifications, strongly enhanced and tunable optical properties and finally have excellent biocompatibility feasible for clinic settings[81]. This is because AuNPs are the most stable of metal nanoparticles and has a long history. Gold extraction started around the 5th millennium B.C. near Bulgaria while by the 1200-1300 B.C. Egypt was extracting roughly 10 tons per year. Soluble gold appeared around the same time that extraction took place, either the 5th or 4th century B.C. in Egypt and China and was used in but aesthetic and curative properties[82]. From here there has been much exploration on how to make and use gold for benefit. Therefor it is not surprising that there have been many advancements in the synthesis of AuNPS such as different shapes and structures, these include: nanorods, silica/gold nanoshells, and hollow AuNPS[83-85]. These wide range of shapes help employ gold into many techniques. However, the there is a large question as to why the gold can give off such a large range of colors. This originates from a basic photophysical response that is not observed in nonmetallic particles. When this metal is exposed to light, it will induce a collective coherent oscillation of free electrons of the metal and will cause the particles on the surface to a charge separation with respect to the ionic lattice. Thus, forming a dipole oscillation along the direction of the electric field of the light. The amplitude of the oscillation will reach a maximum at a specific frequency, this is called surface plasmon resonance or SPR as mention in section 1.6 Dissociation Constants[86-90]. The SPR induces a strong absorption of the incident of light and can be measured

with a Ultra Violet -Visable absorption spectrometer. This band that the SPR reproduces is much stronger in plasmonic nanoparticles, such as gold and silver, than other metals. The band intensity and wavelength is dependent on many factors such as: metal type, particle size, shape, structure, composition and the dielectric constant of the surrounding medium[91]. Essentially the color that is produced by gold reflecting the red light or ~700 nm while the gold nanoparticles absorb the light of the blue-green portion of the spectrum or roughly ~450 nm. Since the gold nanoparticles reflect the ~700 nm, an observation of a red color will be seen. This is one of the main advantages in using gold since it can indicate a bright red color that can be easily seen.

Another advantage is that gold can be easily synthesize, one method that is most common is called the citrate reduction method. This method was first introduced in 1951 by Turkevitch and essentially reduces gold(III) using citrate reduction of $HAuCl_4$ in water[84]. However, this method does not provide a specific size but by variation of the ratio between the reducing and stabilizing agents, gold nanoparticles can be made to a prechosen size between 16 and 147 nm[92]. A variation of this method is used in this study to make gold nanoparticles.

The ease in which gold nanoparticles have a surface modification is a main reason why gold is implemented in a wide range of techniques which have been introduced in previous sections. There are two main ways in which DNA can be conjugated onto the gold surface, these are: absorption, amine coupling via reactive esters, while the third would be layer-by-layer.

In the first where absorption is utilized, gold is considered a self-assembly monolayer (SAMs) and covered in hydroxyl and thiol groups, in which the a sulfur will directly absorb onto the surface of the gold and create a thiol bond. The bonding of this exploits a strong dative bond with a strength that measures roughly 40-50 kcal/mol which is comparable to that of a gold-gold bond[93,94]. This method is typically done as shown below:

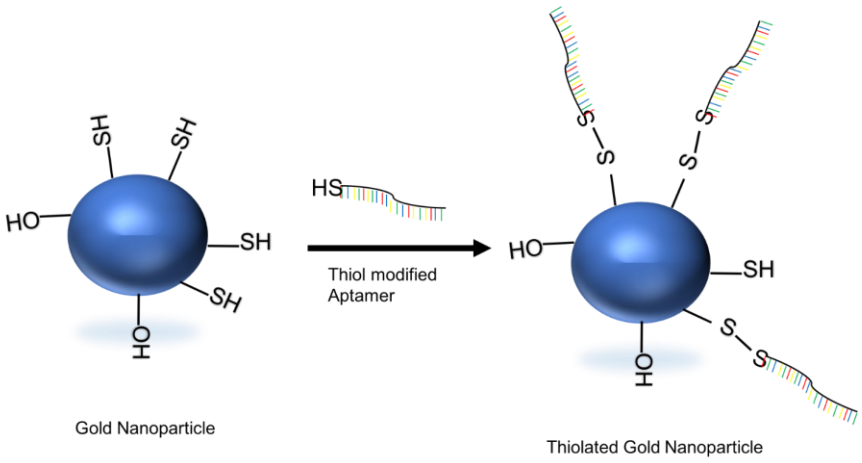

Figure 12. Aptamer Thiolated onto a Gold Nanoparticle Surface

This provides a chemically stable and functional nanoparticle as well as an ease in synthesis therefor it is regularly used. However, it is not the only method and if a stronger bond is desired a different method is used.

A method in which a stronger bond is observed is one in which a covalent bond is produced and is accomplished through the amine coupling via reactive esters. However there a multiple ways in which this is accomplished and depending on how the AuNPs will be modified there are different functional groups adhered to the surface of the gold. Take for instance if a protein was to be conjugated to the surface of the gold, for this to be possible the surface of the gold is coated in a hydrophilic three-dimensional non-cross linked carboxymethylated polymer, making biological reactions to occur in water. This polymer will have a carboxylic acid on its tail. At this point is where the conjugation of the aptamer as long as the aptamer has been modified with an amine group[95].

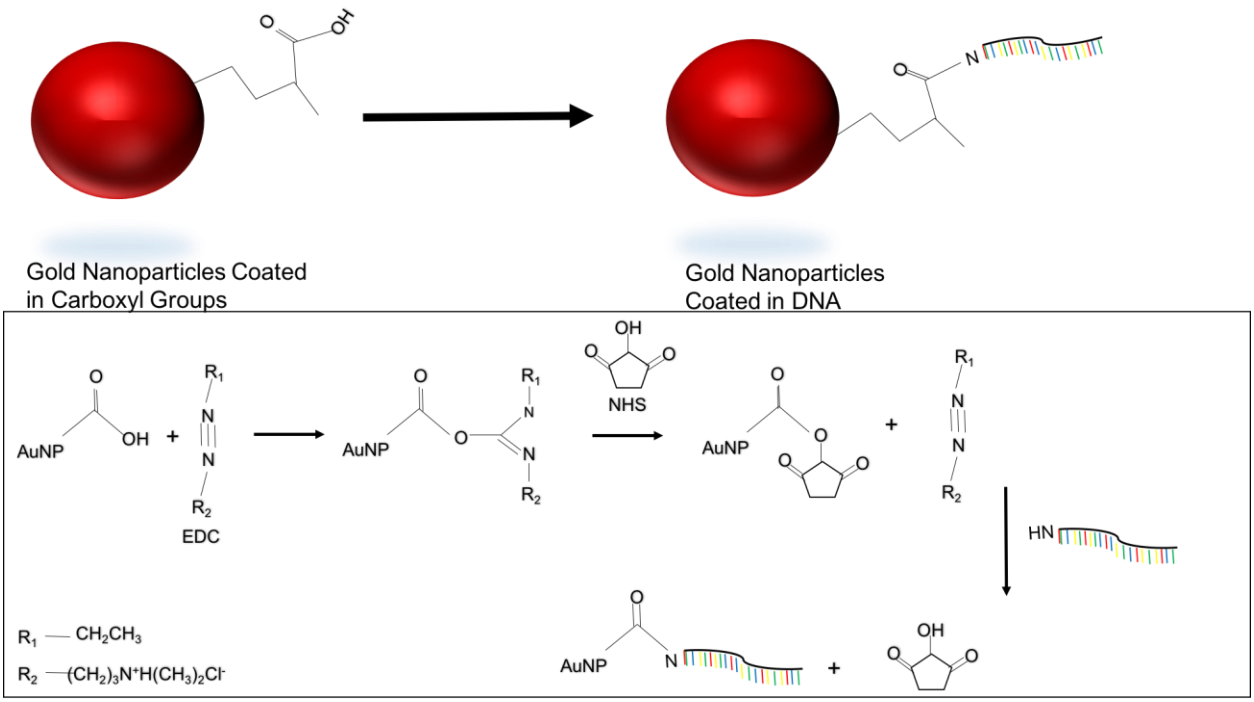

Figure 13. Aptamer Covalently Conjugated onto a Gold Nanoparticle Surface

Even though gold nanoparticles can be easily modified for the use of analytical testing, this is not always necessary. In many cases there has been no need for gold modification for the detection of many types of targets including: 17β-estradiol,[96] metal ions[97,98] adenosine triphosphate[99] and proteins[54,100] .

For these methods are performed in a similar manner. The unmodified gold nanoparticle is incubated with an aptamer that is specific toward the target and will interact with the gold nanoparticle surface. When target is added the aptamer should interact with the target leaving the gold surface open for the salt to interact with the surface allowing for the aggregation of gold nanoparticles leading to a color change as depicted below[101]. A variation of this method will be implemented in this study.

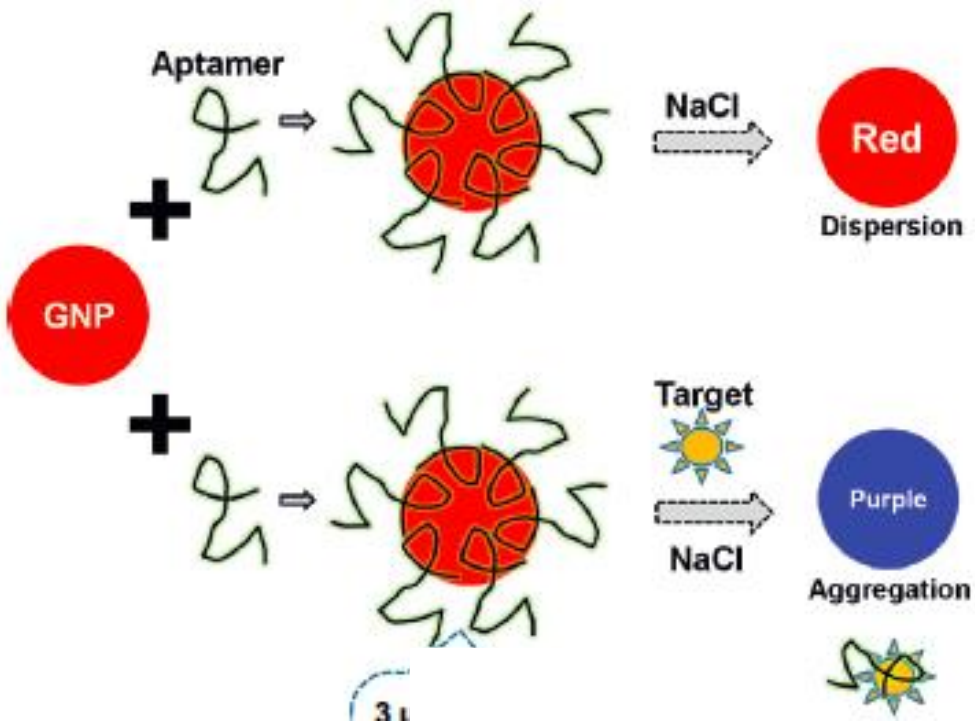

Figure 14. Unmodified Gold Nanoparticle Detection Method

4.2. Materials and Methods

4.2.1. Materials

The materials used in this experiment were purchased from the following, the gold (III) chloride trihydrate ($HAuCl_4$), sodium chloride, and sodium citrate were all purchased from Sigma Aldrich. The carcinoembryonic antigen protein used was purchased from Fitzgerald. While the aptamer used in this experiment was purchased from integrated DNA technologies, with the following sequence: 5' – GGA ATC GGT GGC TTC ATG CTA GTC GCG GGC – 3'

All measurements were taken with Nanodrop 2000/2000c Spectrophotometers and evaluated at the two wavelengths of 520 nm and 650 nm in which the values were ratio.

4.2.2. Preparation of Gold Nanoparticles

The preparation of the AuNPs were made as a previously reported[57]. Briefly, a clean round-bottom flask was incubated with $3HCl{:}1HNO_3$ for at least one hour and rinsed with plenty

of distilled water. In 250 mL of double distilled water, the 50 μL of 50% $HAuCl_4$ was boiled with continuous stirring. When the solution was brought to a boil, 4.5 mL of 4.91 $*10^{-2}$ M of sodium citrate was added to the solution. Then the solution was heated until the color turned to red and was heated for an extra ten minutes. The solution was then cooled to room temperature and then the concentration taken through absorption measurements using Beer Lambert's law with the molar absorptivity (ε) of 2.43 $*10^{8}$ L * mol^{-1} * cm^{-1} and evaluating the absorbance at 520 nm with a 1 cm cuvette.

4.2.3. Detection of Carcinoembryonic Antigen

The detection of CEA was performed by following a previous experiment with some small changes[100]. Briefly, 20 μL of 8μM CEA aptamer 1 was diluted in binding buffer (500 mM NaCl, 2 mM $MgCl_2$, 5 mM KCl, and 1 mM $CaCl_2$) with 360 μL of 5 nM AuNPs. This was incubated at room temperature with gentle mix for forty-five minutes. Then 20 μL of various concentrations of CEA protein was incubated with the AuNP-aptamer1 solution, for thirty minutes with gentle mix at room temperature. To induce the color change, 25 μL of 1 M NaCl was added as indicated in the scheme below.

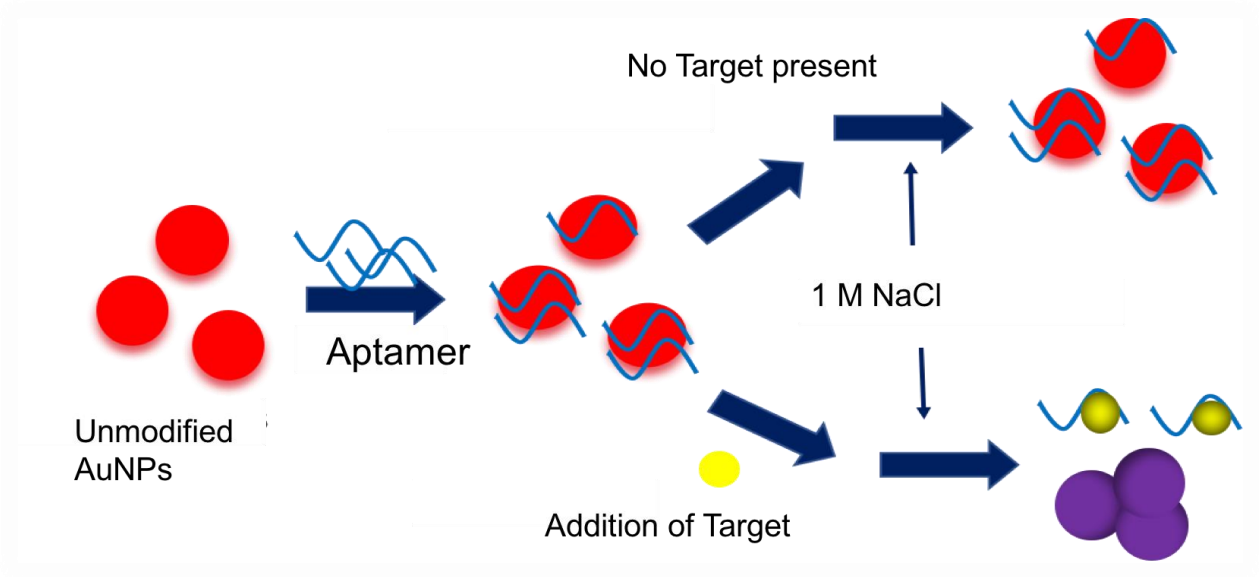

Scheme 3. Representation of the Colorimetric Detection of CEA with Unmodified Gold Nanoparticles and CEA Aptamer 1

The samples were then measured at 520 nm and 650 nm and ratio because when more aggregation present in the solution the higher the signal should be increased at 650 nm and decreased at 520 nm. The data was then plotted in Microsoft excel and given the graphs in the following section.

4.3. Results

To obtain the best results, many conditions needed to be optimized such as: buffer, AuNPs concentration, aptamer-1 concentration, sodium chloride concentration, the aptamer-AuNPs absorption time and the time it takes the aptamer-1 binding to CEA. After the optimal conditions were set a calibration curve was determined along with its limit of detection, dynamic range, and reproducibility of the experiment evaluated as shown in the figures below. These conditions were optimized sequentially while keeping all conditions constant except the condition being evaluated.

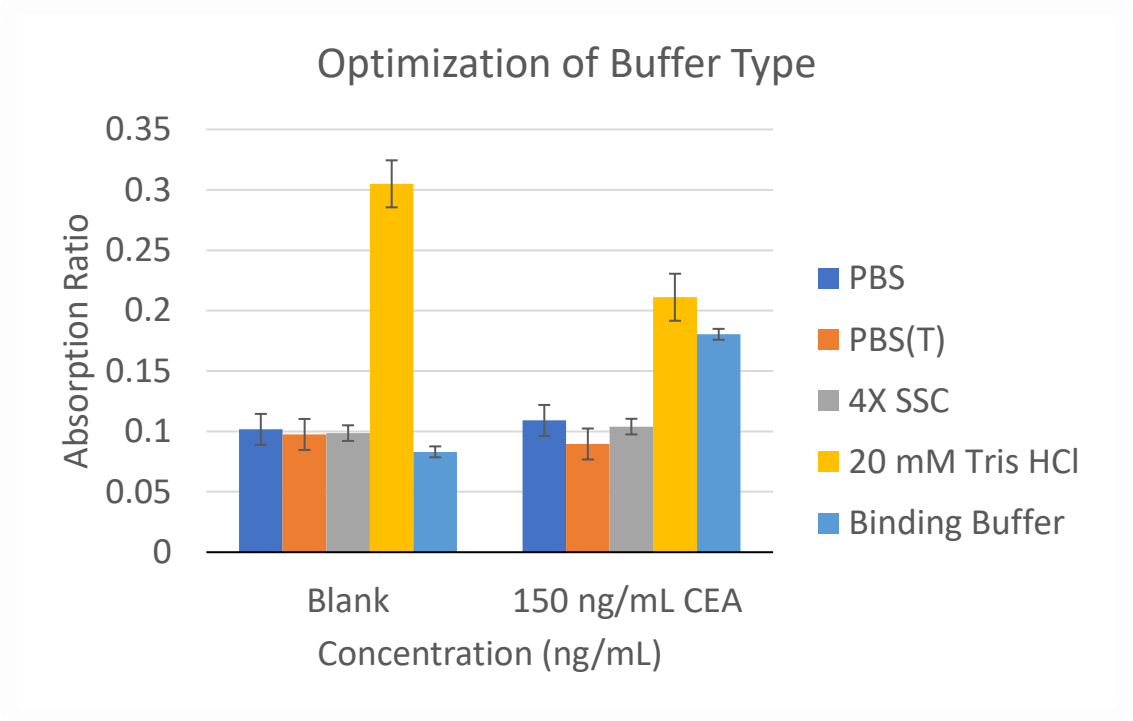

Figure 15. Optimization of Buffer Types

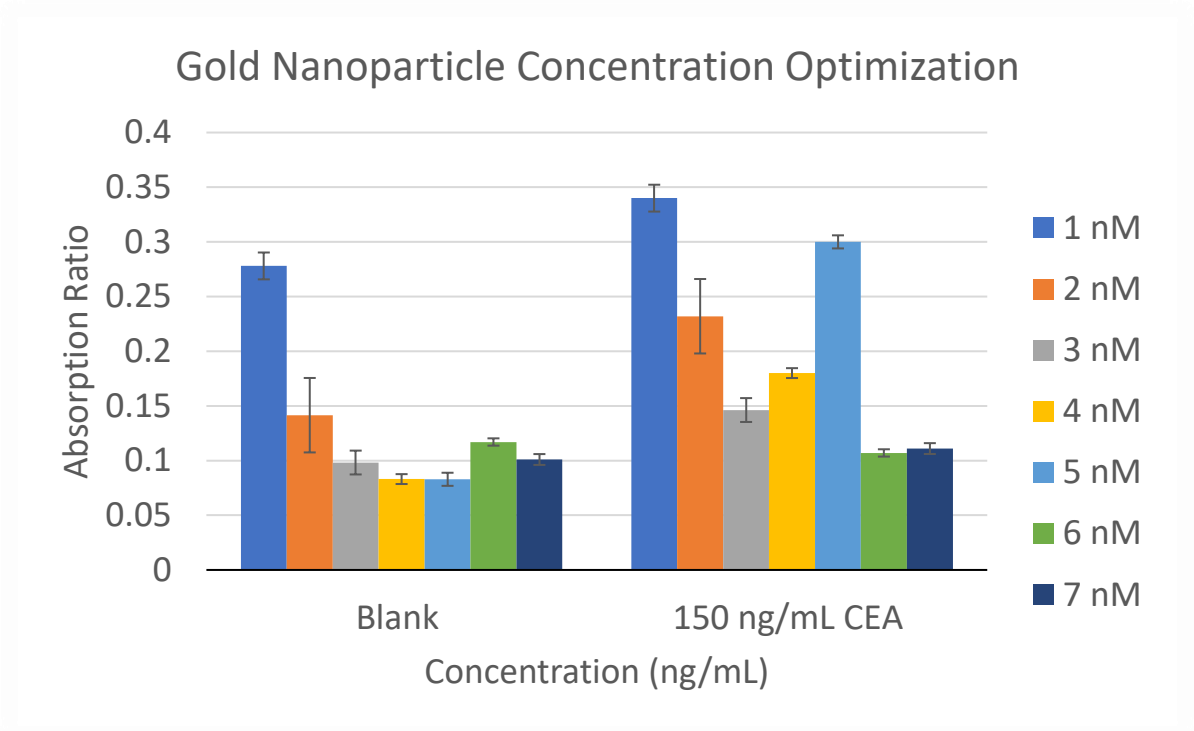

Figure 16. Optimization of Starting Gold Nanoparticle Concentration

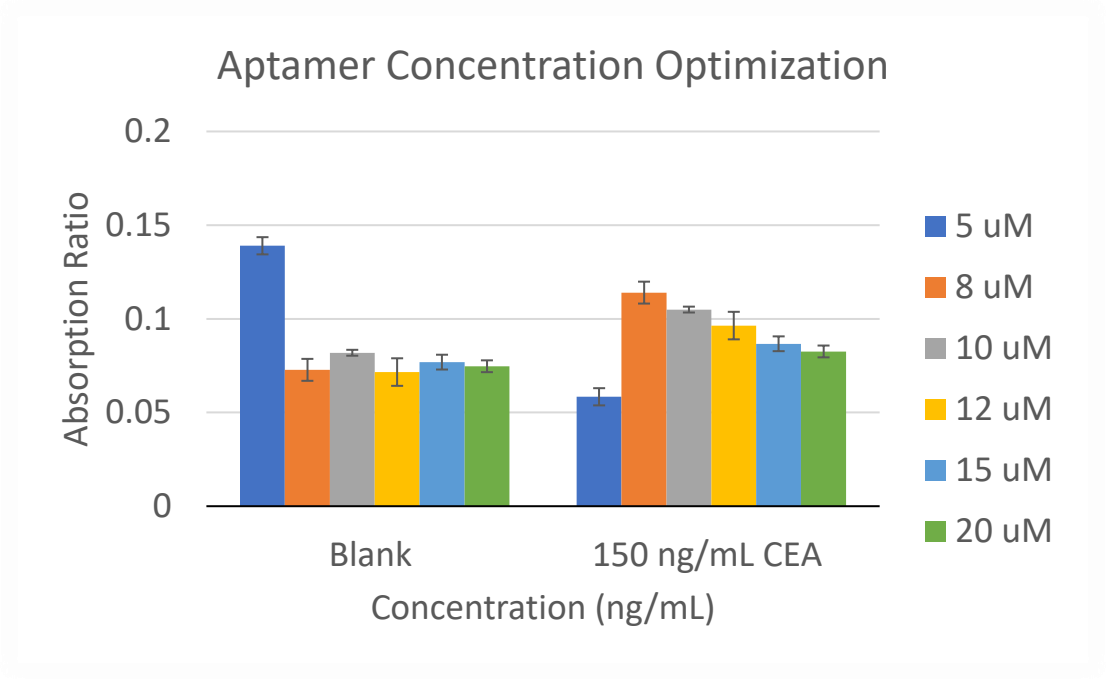

Figure 17. Starting Aptamer Concentration Optimization

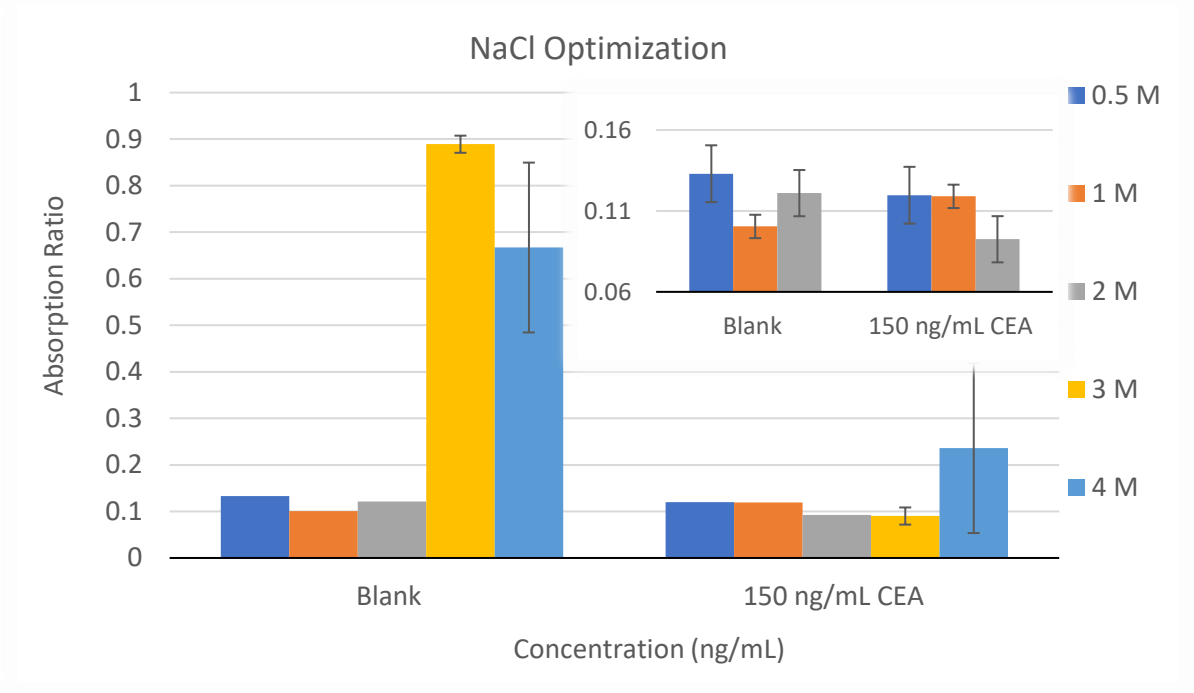

Figures 18. Sodium Chloride Concentration Optimization

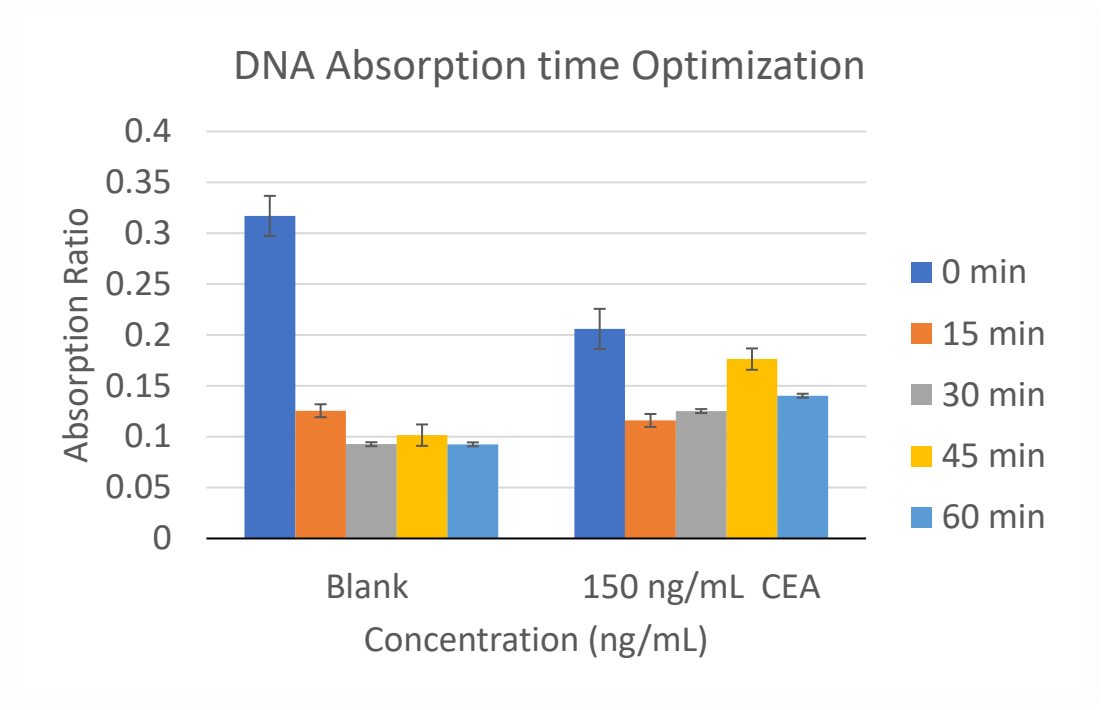

Figure 19. DNA Absorption Time Optimization

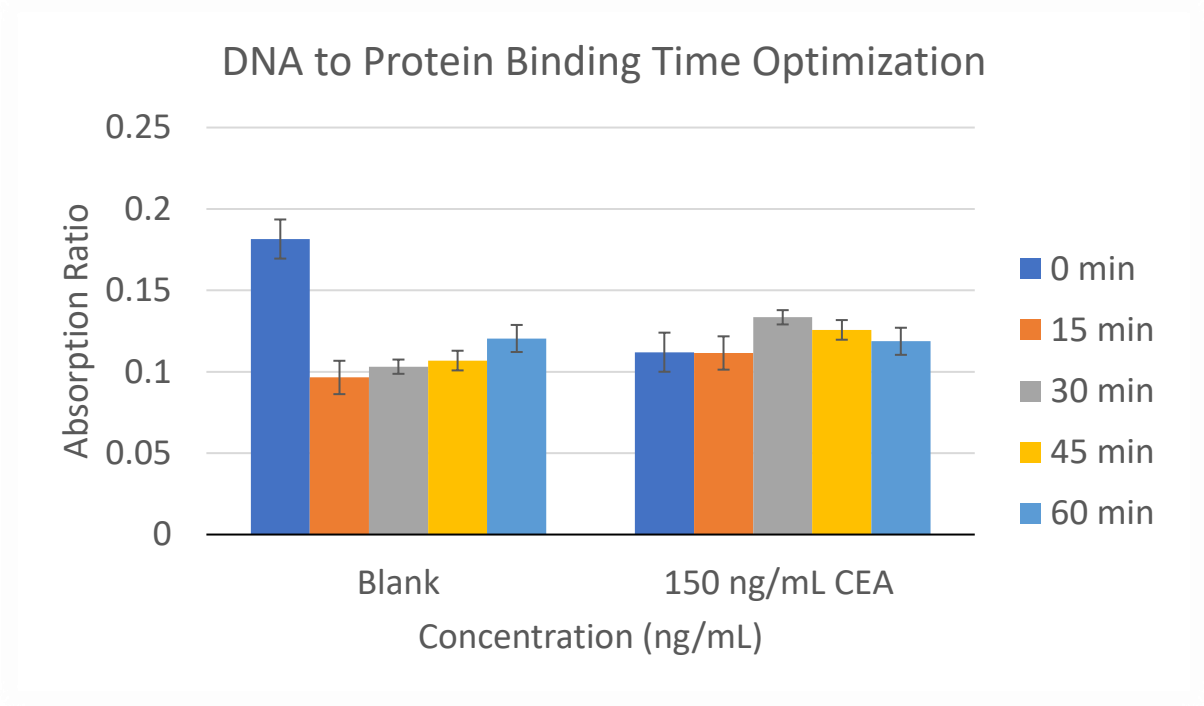

Figure 20. Protein to DNA Binding Time Optimization

Once the optimal conditions were defined, the reproducibility, selectivity and the calibration curve was then accomplished.

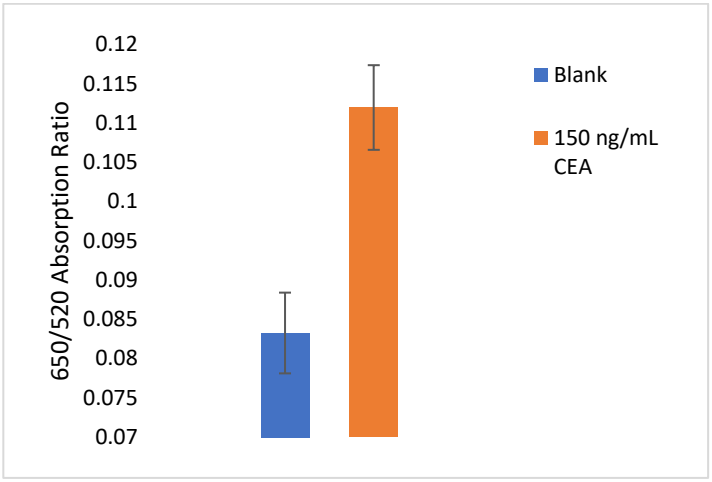

Figure 21. Reproducibility for Colorimetric Test

From the data provided the standard deviation was calculated with the following equation:

Standard Deviation Equation:

$$s = \sqrt{\frac{\Sigma(x - \overline{x})^2}{n - 1}}$$

Sample Calculation of Standard Deviation using 150 ng/mL CEA data:

$$S = \sqrt{\frac{(0.1091 - 0.1120)^2 + (0.1076 - 0.1120)^2 + (0.1076 - 0.1120)^2 + (0.1887 - 0.1120)^2 + (0.112 - 0.112)^2}{5 - 1}} = 0.0054$$

Once the standard deviation was calculated the relative standard deviation was calculated with the following equation:

Relative Standard Deviation Equation:

$$RSD = \left(\frac{standard\ deviation}{average}\right) * 100$$

Sample Calculation of Relative Standard Deviation using 150 ng/mL CEA data:

$$RSD = \left(\frac{0.0054}{0.1120}\right) * 100 = 4.82$$

These calculations were done with both the 150 ng/mL CEA sample and the blank as shown in which the is shown in the table below.

Table 6. Reproducibility of CEA Detection

	Blank	150 ng/mL CEA
Average	0.083	0.112
Standard Deviation	0.0051	0.0053
RSD (%)	6.18	4.82

To ensure that this test is not only reproducible but also that this aptamer is only detecting the CEA protein a selectivity test was also accomplished using carbohydrate antigen 19-9 (CA19-9) at 500 U/mL where the healthy cut-off value of 37 U/mL. With other proteins of bovine serum albumin (BSA) and human immunoglobulin G (IgG) at 50 nM of each protein.

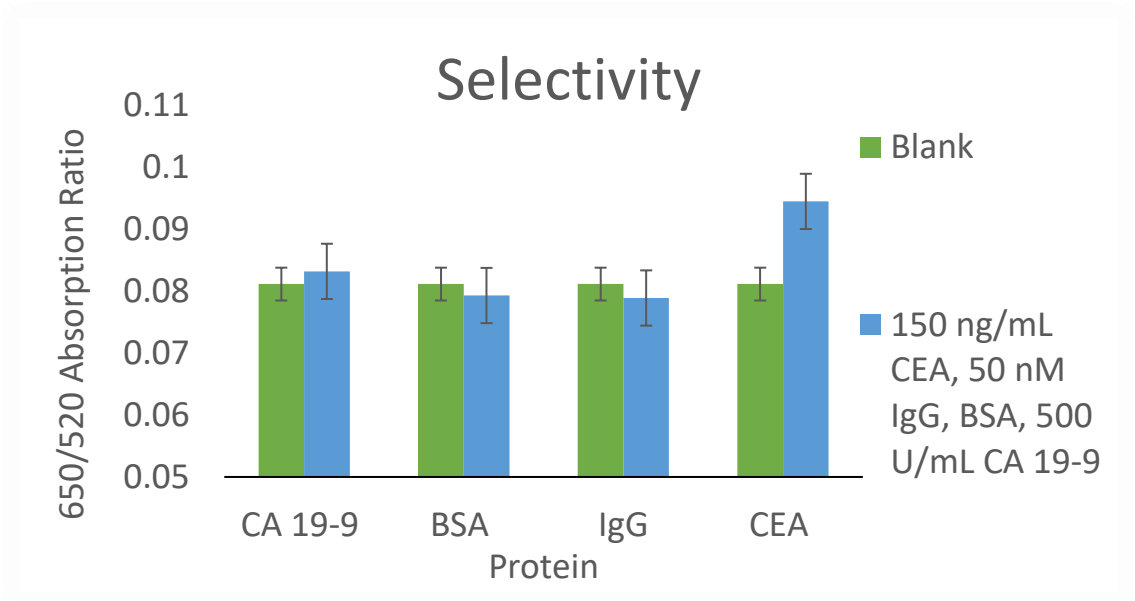

Figure 22. Selectivity for CEA Colorimetric Test

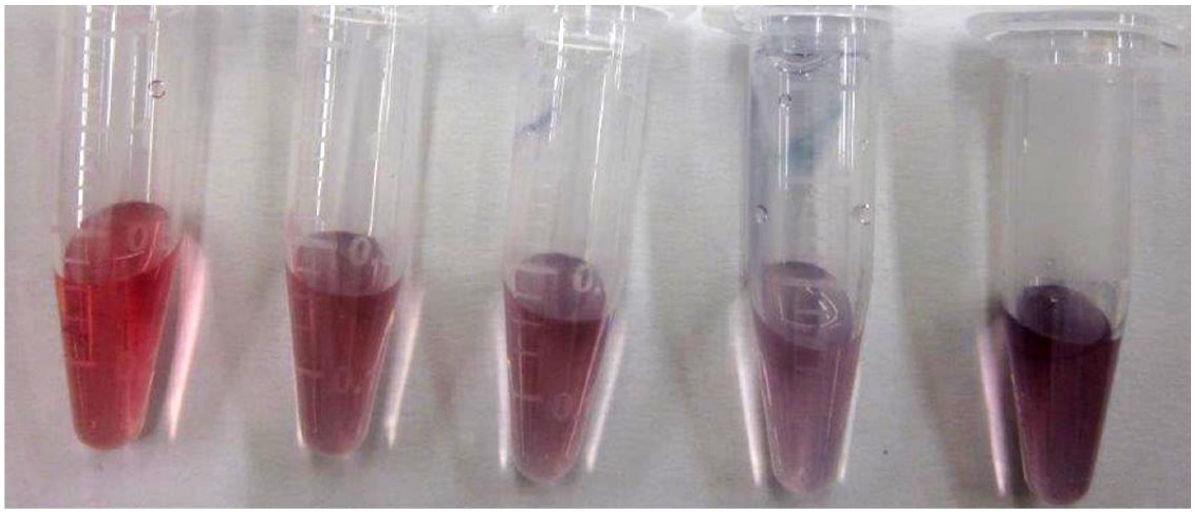

Figure 23. Depiction of Color change in Colorimetric Test

In figure 24 the following concentrations were tested from left to right: Blank, 50 ng/mL, 100 ng/mL, 200 ng/mL and 400 ng/mL CEA.

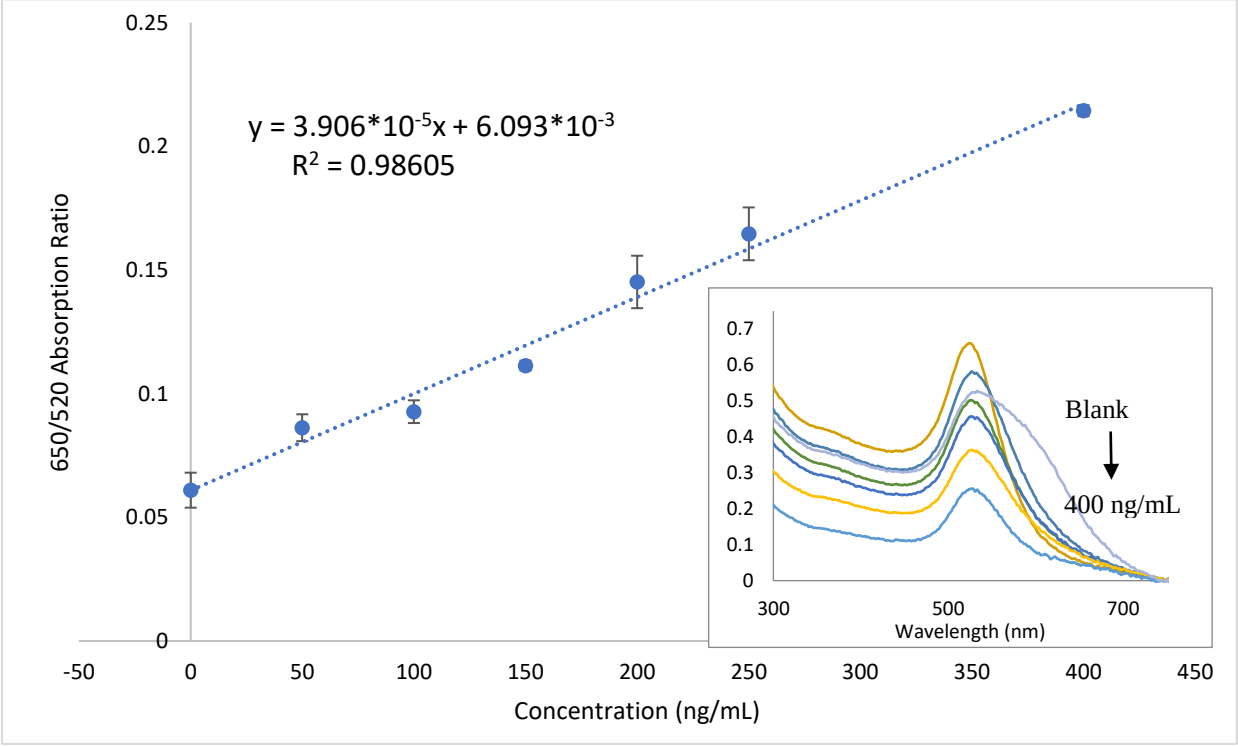

Figure 24. Calibration Curve for Aptamer One in Gold Colorimetric Test

From the calibration curve the linear regression was fitted with a line y=0.004x +0.0609 in which allowed for the calculation of limit of detection in the following manner:

Limit of Detection Calculation:

$$LOD = \frac{3 * s_{bl}}{m}$$

Sample Calculation

$$LOD = \frac{3 * 0.0071}{0.003906} = 54.31\ ng/mL$$

4.4. Discussion

In this experiment, a new aptamer was implemented for the detection of carcinoembryonic antigen protein with the use of unmodified gold nanoparticles for a simple colorimetric test. In order to get the best results, many parameters needed to be optimized. The parameters were optimized sequentially and were chosen based on the difference between the blank and actual signal. The first condition that was optimized was the type of buffer. The buffers that were tested were PBS, PBS(T), SSC, 20 mM Tris HCl and finally a binding buffer with the components of 500 mM NaCl, 2 mM $MgCl_2$, 5 mM KCl, and 1 mM $CaCl_2$. As clearly shown in figure 15, binding buffer had the best response, while the other buffers such as PBS, PBS(T) and SSC did not provide the proper environment to induce a color change when protein was present while tris HCl provided to high of background. Then the starting concentration of gold nanoparticles were tested starting form 1 nM to 7 nM in which 5 nM had the best response. The amount of aptamer concentration was also optimized by testing the following concentrations 5, 8, 10, 12, 15, 20 μM. Figure 16 clearly indicates that 8 μM had the best response. Even though 10 μM had a similar response, the 8 μM had a lower noise ratio which is why it was chosen. The amount of salt added to the solution is vitally important since it is what will induce the color

change. Therefor the concentrations of 0.5, 1, 2, 3, and 4 M were tested. At higher than 2 M the noise from the blank became exceptionally high, however zooming in on the samples 0.5, 1 and 2 M in figure 18, indicated that 1 M was the best concentration of salt to use. Incubation times were also very important, and thus the amount of time for the aptamer to absorb onto the gold surface was tested starting with 0 to 60 minutes for fifteen minute intervals. As shown in figure 19, 45 minutes was the optimal time, even though after 15 minutes the noise from the blank was greatly decreased but the greatest difference was shown in the 45 minutes therefor 45 minutes was the optimal time for the DNA absorption time onto the gold surface. Finally, the time it took for the interaction between DNA and protein to bind was also optimized where figure 20 clearly depicts that 30 minutes was the optimal time. After all the parameters were optimized lead to the experiment with the following conditions: each test should be accomplished in binding buffer with starting with 360 μL 5 nM of AuNPs with 20 μL of 8 μM and incubating for 45 minutes at room temperature. Then 20 μL of various amounts of concentration of protein was added and incubated for a further 30 minutes at room temperature. In the final step there was 25 μL of 1 M NaCl. The color change could then be visualized and quantified using Nanodrop 2000/2000c Spectrophotometers.

The color change was induced when the 1 M NaCl solution was added because salt can shield the negative charge on the gold nanoparticles allowing the particles to become closer together and aggregate. Upon aggregation, the size and shape of the gold nanoparticles change thus changing the color of the solution. Without the addition of salt the repulsion forces between the particles are too strong for the gold to aggregate[102]. When no protein of CEA is present, the aptamer could stabilize the AuNPs thus keeping the red color however when the CEA was present the aptamer having a higher binding affinity toward the protein would stop interacting

with the AuNPs and bind with the protein thus allowing for the distance between the AuNPs to shorten, causing aggregation and thus leading to a change of color from a red to purple. This change in color is gradual depending on the concentration of CEA present as demonstrated in figure 23.

Once the conditions were optimized the question of if this test is reproducibly became apparent. This was done by repeating the test five different times in triplicate form under the optimal conditions previously described. Then the relative standard deviation was calculated giving the test of less than 10% indicating that this test is indeed reproducible and stable. This method should give then same results multiple times.

Once the method proved to be reproducible the calibration curve was then determined as shown in figure 24. This test provided to have a limit of detection of visually with 50 ng/mL of CEA as shown in figure 23, however by measuring the absorption ratio of 650/520 and plotting a linear trend was observed from 0 to 400 ng/mL of CEA. By fitting the curve the limit of detection was calculated to be 54.31 ng/mL of CEA by taking the average of blank plus three times the standard deviation. With a healthy cut-off value of CEA in regular patients to be 5 ng/mL this method has proven to not be very sensitive. However, this shows promise that the aptamer can be implemented in other techniques. There are other analytical methods in which aptamers can be implemented in such as fluorescence, chemiluminescence, or even electrochemical.

Since the test has proven to be reproducible, another question that is typically asked is, is this aptamer selective and can it definitively detect CEA when no other protein are present. Since multiple negative selection rounds were performed in the graphene oxide SELEX, this aptamer should be selective however, it is should be verified. The proteins carbohydrate antigen 19-9 (CA

19-9), bovine serum albium (BSA) and human IgG were tested. Figure 22 indicates that there are no large response to other proteins even when there were large concentrations of other protein present. This indicates that the aptamer is selective toward CEA.

4.5. Conclusion

In conclusion, this method has proven successful in implementing the newly designed aptamer specific toward CEA for an easy detection of CEA with a linear range from 50 ng/mL to 400 ng/mL of CEA and a calculated limit of detection of 54.3 ng/mL CEA and a visual detection of 50 ng/mL. This is the first test in which this aptamer has been implemented and shows much promise for future analytical and potentially point-of-care testing of CEA. Another potential future possibility is to combine the aptamer used in this study with another aptamer that has been reported to implement in a sandwich sort of assay. Either way the future applications for this aptamer are endless.

CHAPTER 5. CONCLUSION

This thesis was broken down into three sections, the first was to identify an aptamer specific towards carcinoembryonic antigen (CEA) using graphene oxide assisted SELEX. In that portion of the experiment an aptamer was identified based on frequency of number of sequences found by NexGen Sequencing. Aptamer one was the aptamer had the highest number of appearances and was thus used for future experiments.

The second part of this experiment was to calculate the dissociation constant for the aptamer that had been previously identified using surface plasmon resonance (SPR) and to compare that value with an aptamer that had already been identified with a different SELX method. This was done for two reasons, the first was quantify the quality of the aptamer identified and the second was to directly compare aptamer one to the reported aptamer. The dissociation constant for the reported aptamer was found to be 828.26 ± 23.99 nM while the aptamer isolated with the graphene oxide assisted SELEX was found to be 253.68± 15.75 nM. This indicates that the aptamer isolated from the GO-SELEX binds more tightly to CEA than the aptamer isolated from the affinity-SELEX, thus graphene oxide can sufficiently separate the specific from the non-specific strands indicating that this GO-SELEX could be used for future experiments.

In the final part of this experiment was to successfully implement aptamer one for the detection of CEA using unmodified gold nanoparticles. This method was proven to successfully detect CEA by evaluating a simple color change. This method provided a linear range from 50 ng/mL to 400 ng/mL of CEA and a calculated limit of detection of 54.3 ng/mL CEA and a visual detection of 50 ng/mL. This is the first test in which this aptamer has been implemented and shows much promise for future analytical and potentially point-of-care testing of CEA.

This experiment was successful for a starting off point for many future experiments, such as performing the graphene-oxide assisted SELEX for other proteins such as carbohydrate antigen 19-9 (CA 19-9), complementary factor B (CFB), and C4BP**α**, which are common biomarkers for pancreatic cancer. There are also a lot of potential for the use of the aptamer that has been identified, since the limit of detection was so poor, it would be easy to implement this aptamer in other analytical techniques such as fluorescence, chemiluminescent and electrochemical. Another potential future possibility is to combine the aptamer one used with a reported aptamer to implement in a sandwich assay for point of care diagnositcs. Either way the future applications for this aptamer are endless.

REFERENCES

1) Gold, P.; Freedman, S. Demonstration of Tumor-Specific Antigens in human Colonic carcinomata by immunological tolerance and absorption Techniques. *J. Exp Med.* **1965,** *122,* 467-481.

2) Hammarstrom, S. The carcinoembryonic antigen (CEA) family: structures, suggested functions and expression in normal and malignant tissues. *Cancer Biology.* **1999,** *9*, 67-81.

3) Olsen, A.; Teglund, S.; Nelson, D.; Gordon, L.; Copeland, A.; Georgescu, A.; Carrano, A.; Hammarstrom, S. Gene Organization of the Pregnancy-Specific glycoprotein region on human chromosome 19: Assembly and Analysis of 700-Kb cosmid contig spanning the region. *Genomics,* **1994,** *23,* 659-668.

4) Paxton, R.J.; Mooser, G.; Pande, H.; Lee, T.D.; Shively, J. E. Sequence analysis of carcinoembryonic antigen: identification of glycosylation sites and homology with the immunoglobulin supergene family. *Proc. Natl. Acad. Sci.* **1987,** *84,* 920-924

5) Moertel, C. G.; O'Fallon, J. R.; Go, V. L. W.; O'Connell, M. J.; Thynne, G. S. The Preoperative Carcinoembryonic Antigen Test in Diagnosis, Staging, and Prognosis of Colorectal Cancer. *Cancer.* **1986.** *58,* 603-610.

6) Luong, J.; Vashist, SK. Immunosensing procedures for carcinoembryonic antigen using graphene and nanocomposites. Biosensors Bioelectronics **(20015).** 10.1016/j.bios.2015.11.053

7) Chritenson, R. H.; Cervelli, D. R.; Sterner, J.; Bachmann, K. M.; Rebuck, H.; Gray, J.; Kelley, W. E. Analytical Performance and clinical concordance of the cancer biomarkers CA 15-3, CA 19-9, CA 125II, Carcinoembryonic Antigen, and Alpha-Fetoprotein on the Dimension Vista System. *Clinical Biochemistry.* **2011,** *44*, 1128-1136.

8) Grunnet, M.; Sorensen, J. B. Carcinoembryonic antigen (CEA) as tumor marker in lung cancer. *Lung Cancer.* **2012.** *76,* 138-143.

9) Hammarstrom, S. The carcinoembryonic antigen (CEA) family: structures, suggested functions and expression in normal and malignant tissues. *Cancer Biology.* **1999,** *9*, 67-81.

10) Clark Jr., L.C.; Lyons, C. Ann. N. Y. Electrode Systems for continuous monitoring in cardiovascular surgery. *Acad. Sci.,* **1962,** *102* 29–45

11) Lai, G.; Yan, F.; Ju, H.; Dual Signal Amplification of glucose oxidase-functionalized Nanocomposites as a trace label for ultrasensitive simultaneous multiplexed electrochemical detection of tumor markers. *Anal. Chem.* **2009,** *81,* 9730-9736.

12) Huang, K.J.; Niu, D.J.; Xie, W.Z.; Wang, W. A disposable electrochemical immunosensor for Carcinoembryonic Antigen based on nano-Au/multi-walled carbon nanotubes-chitosans nanocomposite film modified glassy carbon electrode. *Analytic Chimica Acta.* **2010.** *659,* 102-108.

13) Wilson, M.S. Electrochemical Immunosensors for the Simultansous Detection of Two Tumor Markers. *Anal. Chem.* **2005.** *77,* 1496-1502.

14) Lao, U.L.; Mulchandani, A.J.; Chen, W. Simple Conjugation and Purification of Quantum dot-Antibody Complexes using a thermally responsive elastin-Protein L Scaffold as immune-fluorescent agents. *J. Am. Chem. Soc.* **2006,** *128,* 14756-14757.

15) Fu, Z.; Yan, F.; Liu, H.l Yang, Z.; Ju, H. Channel –resolved multi-analytic immune-sensing system for flow-through chemiluminescent detection of α-fetoprotein and carcinoembryonic antigen. *Biosensors and Bioelectronics.* **2008.** *23,* 1063-1069.

16) Tang, H.; Chen, J.; Nie, L.; Kuang, Y.; Yao, S. A label-free electrochemical immunoassay for carcinoembryonic antigen (CEA) based on gold nanoparticles (AuNPs) and non-conductive polymer film. *Biosensors and Bioelectronics.* **2007,** *22,* 1061-1067

17) Liu, M; Jia, C.; jin, Q.; Lou, X.; Yao, S.; Xiang, J. Novel Colorimetric enzyme immunoassay for the detection of carcinoembryonic antigen. *Talanta,* **2010.** *81,* 1625-1629

18) Lakhin, A.V.; Tarantul, V.Z.; Gening, L.V. Aptamers: Problems, Solutions and Prospects. Acta. Naturae. 2013. 5, 34-42.

19) Ellingtion A.D.; Szostak J.W. in vitro selection of RNA molecules that bind specific ligands. *Nature.* 346, 818-822. 1990. Doi: 10.10381346818a0

20) Kulbachinskiy, A.V. Review: Methods for Selection of Aptamers to Protein Targets. *Biochemistry.* **2007.** *72,* 1505-1581.

21) Xiong, X.; Lv, Y.; Chen, T.; Zhang, X.; Wang, K.; Tan, W. Nucleic Acid Aptamers for Living Cell Analysis. *Annu. Rev. Anal. Chem.* **2014.** *7,* 405-426.

22) Stoltenburg, R.; Reinemann, C.; Strehlitz, B. Selex-a revolutionary metho to generate high-affinity nucleic acid ligands. *Biomolecular engineering.* **2007.** *24,* 381-403.

23) Bouchard, P.R.; Hutabarat, R.M>; Thompson, K.M. Discovery & Development of Therapeutic Aptamers. *Annual. Rev. of Pharmacol. & Toxicol.* **2010.** *50,* 237-257.)

24) Keefe, AD.; Pai, S.; Ellington, A. Aptamers as therapeutics. *Nat. Rev. Drug Discon.* **2010.** *9,* 537-550

25) Parashar, A. Aptamers in Therapeutics. *Journal of Clinical and Diagnostics Research.* **2016.** DOI:10.7860/JCDR/2016/18712.7922

26) Siddiqui, M.A.; Keating, G.M. Polyethylene glycol (PEG)-conjugated, modified synthetic RNA oligonucleotide and aptamer; selective vascular endothelial growth factor (VEGF) antagonist. *Drugs.* **2005.** *65,* 1571-1579.

27.) Vinores SA. Pegaptanib in the treatment of wet, age-related macular degeneration. *Int J Nanomedicine*. **2006**. *1(3),* 263-68).

28.) Mendonsa SD, Bowser MT. Invitro Evolution of functional DNA using capillary electrophoresis. *J Am Chem Soc*. **2004,** *126(1),* 20-21).

29.) Gould HJ, Sutton BJ, Beavil AJ, Beavil RL, McCloskey N, Coker HA, et al. The biology of IGE and the basis of allergic disease. *Annu Rev Immunol.* **2003**, *21*, 579-28.

30.) Kim YM, Choi KH, Jang YJ, Yu J, Jeong S. Specific modulation of the antiDNA autoantibody-nucleic acids interaction by the high affinity RNA aptamer. *Biochem Biophys Res Commun.* **2003,** *300(2),* 516-23

31.) Lee SW, Sullenger BA. Isolation of a nuclease–resistant decoy RNA that selectively blocks autoantibody binding to insulin receptors on human lymphocytes. *J Exp Med*. **1996,** *184,* 315-24.

32.) Oberthür D, Achenbach J, Gabdulkhakov A, Buchner K, Maasch C, Falke S, et al. Crystal structure of a mirror-image L-RNA aptamer (Spiegelmer) in complex with the natural L-protein target CCL2. *Nat Commun.* **2015,** *6,* 6923.

33.) Pietras K, Rubin K, Sjoblom T, Buchdunger E, Sjoquist M, Heldin CH, et al. Inhibition of platelet-derived growth factor receptors reduces interstitial hypertension and increases transcapillary transport in tumours. *Cancer Res.* 2**001,** *61*, 2929-34.

34.) Pietras K, Rubin K, Sjoblom T, Buchdunger E, Sjoquist M, Heldin CH, et al. Inhibition of PDGF receptor signaling in tumour stroma enhances antitumour effect of chemotherapy. C*ancer Res*. **2002**, *62*, 5476-84.

35.) Green LS, Jellinek D, Jenison R, Ostman A, Heldin CH, Janjic N. Inhibitory DNA ligands to platelet derived growth factor B-chain. *Biochemistry.* **1996,** *35(45),* 14413-24

36) Blank M, Weinschenk T, Priemer M, Schluesener H. Systematic evolution of a DNA aptamer binding to rat brain tumour microvessels selective targeting of endothelial regulatory protein pigpen. *J Biol Chem*. **2001**, *276,* 16464-68.

37) Herrmann A, Priceman SJ, Swiderski P, Kujawski M, Xin H, Cherryholmes GA, et al. CTLA4 aptamer delivers STAT3 siRNA to tumour-associated and malignant T cells. *J Clin Invest*. **2014**, *124(7),* 2977-87.

38) Herold-Mende C, Mueller MM, Bonsanto MM, Schmitt HP, Kunze S, Steiner HH. Clinical impact and functional aspects of tenascin-C expression during glioma progression. *Int J Cancer*. **2002**, *98(3),* 362-69.

39) Hicke BJ, Marion C, Chang YF, Gould T, Lynott CK, Parma D, et al. Tenascin-C aptamers are generated using tumour cells and purified protein. *J Biol Chem.* **2001**, *276*, 48644-54.

40.) Schmidt KS, Borkowski S, Kurreck J, Stephens AW, Bald R, Hecht M, et al. Application of locked nucleic acids to improve aptamer invivo stability and targeting function. *Nucleic Acids Res.* **2004**, *32*, 5757-65.

41.) Dion DA, Chen H, Hicke BJ, Swiderek KM, Gold L. A tenascin-C aptamer identified by tumour cell SELEX: Systematic evolution of ligands by exponential enrichment. *PNAS*. **2003,** *100(26),* 15416-21.

42.) Jeong S, Eom T, Kim S, Lee S, Yu J. Invitro selection of the RNA aptamer against the Sialyl Lewis X and its inhibition of the cell adhesion. *Biochem Biophys Res Commun*. **2001**, *281*, 237-43

43.) Carter RE, Feldman AR, Coyle JT. Prostate-specific membrane antigen is a hydrolase with substrate and pharmacologic characteristics of a neuropeptidase. *Proc Natl Acad Sci USA*. **1996**, *93(2)*, 749-53.

44.) Pinto JT, Suffoletto BP, Berzin TM, Qiao CH, Lin S, Tong WP, et al. Prostatespecific membrane antigen: a novel folate hydrolase in human prostatic carcinoma cells. *Clin Cancer Res.* **1996,** *2(9)*, 1445-51.

45.) Lapidus RG, Tiffany CW, Isaacs JT, Slusher BS. Prostate-specific membrane antigen (PSMA) enzyme activity is elevated in prostate cancer cells. *Prostate.* **2000**, *45(4)*, 350-54.

46.) Burger MJ, Tebay MA, Keith PA, Samaratunga HM, Clements J, Lavin MF, et al. Expression analysis of delta-catenin and prostate-specific membrane antigen: their potential as diagnostic markers for prostate cancer. *Int J Cancer*. **2002,** *100(2),* 228-37.

47.) Lupold SE, Hicke BJ, Lin Y, Coffey DS. Identification and characterization of nuclease-stabilized RNA molecules that bind human prostate cancer cells via the prostate-specific membrane antigen. *Cancer Res.* **2002**, *62,* 4029-33.

48.) Christian S, Pilch J, Akerman ME, Porkka K, Laakkonen P, Ruoslahti E. Nucleolin expressed at the cell surface is a marker of endothelial cells in angiogenic blood vessels. *J Cell Biol.* **2003,** *163*, 871-78.

49.) Bates PJ, Laber DA, Miller DM, Thomas SD, Trent JO. Discovery and development of the G-rich oligonucleotide AS1411 as a novel treatment for cancer. *Exp Mol Pathol.* **2009**, *86(3),* 151-64.

50) Smith, C.L. Compositions comprising nucleic acid aptamers. US 20100254901 A1, October 7, 2010

51) Turek, C.; Gold, L. Systematic evolution of ligands through exponential enrichment: RNA lignads to bacteriophage T4 DNA polymerase. *Science.* **1990.** *249(4968),* 505-10.

52) Liu, C.; Liu, X.; Qun, Y.; Deng, C.; Xiang, J. A simple regenerable electrochemical aptasensor for the parallel and continuous detection of biomarkers. *RCS Adv.* **2016.** *6,* 58469-58476

53) Pan, L.; Zhao, J.; Huang, Y.; Zhao, S.; Liu, Y. Aptamer-based microchip electrophoresis assays for amplification detection of carcinoembryonic antigen. *Clinica Chimica Acta.* **2015.** *450,* 304-309

54) Luo, Ch.; Wen, W.; Lin, F.; Zhang, X.; Gu, H.; Wang, S. Simplified aptamer-based colorimetric method using unmodified gold nanoparticles for the detection of carcinoma embryonic antigen. *RSC Adv.* **2015.** *5,* 10994-10999

55) He. Y.; Chai, Y.; Wang, H.; Bai, L.; Yaun, R. A signal-on electrochemiluminescence aptasensor based on the quenching effect of manganese dioxide for sensitive detection of carcinoembryonic antigen. *RSC. Adv.,* **2014,** *4,* 56756-56761

56) Zeng, X.; Ma, S.l Bao, J.; Tu, W.; Dai, Z. Using Graphene-Based Plasmonic Nanocomposites to Quench Energy from Quantum Dots f0r Signal-On Photoelectrochemical Aptasensor. *Analytical Chemisry.* **2013,** *83,* 11720-11724.

57) Shi, G.; Cao, J.; Zhang, J.; Huang, K.; Liu, Y.; Chen, Y.; Ren, S. Aptasensor based on tripetalous cadmium sulfide graphene electrochemiluminescence for the detection of carcinoembryonic antigen. *Analyst.* **2014,** *139,* 5827-5834.

58) Lin, Z.; Zhang, G.; Yang, W.; Qiu, B.; Chen, G. CEA Fluorescence biosensor based on the FRET between polymer dots and Au nanoparticles. *Chem Commun.,* **2012,** *48,* 9918-9920.

59) Gariepy, J.; Huang, E.; Orava, E.; Revers, L. Aptamer specific to CEA and tnf-aplpha and their therapeutic uses. WO 2013185241 A1, December 19, 2013

60) Szeto, K.; Latalippe, DR. ; Ozar A; Pagano, J.M.; White, B.S. Shalloway, D.J.; Lis, J.T.; Craighead, H.G. Rapid-SELEX for RNA Aptamers. *PLOS ONE.* **2013.** V8, I12. E82667

61) Yuce, M.; Ullan N.; Budak, H. Trends in aptamer selection methods and applications. *Analyst.* **2015.** 140 5379.

62) Mendonsa, S.D; Bowser, M.T. In vitro Selection of Aptamers with Affinity for neuropeptide Y using capillary electrophoresis. *J. Am. Chem. Soc.* **2005.** *127* 9382-9383

63) Lautner, G.; Balogh, A.; Bardoczy, V.; Meszaros T.; Gyurcsanyi, R.E. Aptamer-based biochip for label-free detection of plant virus coat proteins by SPR imaging. *Analyst.* **2010,** *135*, 918-926.

64) Jing, M. and Bowser, M.T. Isolation of DNA aptamers using micro-free electrophoresis. *Lab Chip.* **2011.** *11,* 3703-3709

65) Cox J.C., Ellington, A.D. Automated Selection of Anti-Protein Aptamers. *Bioorganic and Medicinal Chemistry***. 2001.** *9* 2525-2531

66) Cox, J.C.; Hayhurst A.; Hesselberth, J. Bayer T.S.; Georgiou and Ellington, D. Automated selection of aptamers against protein tagets translated in vitro: from gene to aptamer. *Nucleic Acids Research.* **2002** *30***,** 1-14.

67) Nitsche, A.; Kurth, A.; Dunkhorst, A.; Panke, O.; Sielaff, H.; Jung, W.; Muth, D.; Scheller, F.; Stocklein, W.; Dahmen, C.; Paul, G.; Kage, A. One-step selection of Vaccinia Virius-binding DNA aptamers by MonoLEX. *BMC Biotechnology* **2007.** *7*, 48-60.

68) Cao, L.L.; Cheng, L.W.; Zhang, Z.Y.; Wang, Y.; Zhang, X.X. Visual and high-throughput detection of cancer cells using graphene oxide-based FRET aptasensing microfluidic chip. *Lab Chip.* **2012.** *12,* 4864-4869.

69) Park, J.; Tatavarty, R.; Kim, D.W.; Jung, H.; Gu, M.B. Immobilization-free screening of aptamers assisted by graphene oxide. *Chem Commun.* **2012.** *48* 2071-2073.

70) Demarse, N.; Quinn, C. Determination of a Protein ligand interaction via continuous isothermal titration calorimetry. *TA Instruments.* **2011.** 1-6

71) Liang, Y. Applications of isothermal titration calorimetry in protein science. *Acta. Biochem. Biophys. Sin.* **2008**. *40* 565-576.

72) Kozlov, A.G.; Lohman, T.M. SSB Binding to ssDNA Using Isothermal Titration Calorimetry. *Methods Mol Biol.* **2012.** *922,* 37-54

73) Cliff, MJ,; Gutierrez A.; Ladbury, JE. A survey of the year 2003 literature on applications of isothermal titration calorimetry. *J. Mol. Recognit.* **2004.** *17,* 513-523.

74) Jing, M.; Bowser, M.T. A Review of Methods for Measuring Aptamer-ProteinEquilibria. *Anal Chim Acta.* **2011** *686,* 9-18.

75) Sipova, H.; Homola, J. Surface Plasmon resonance sensing of nucleic acids: A review. *Analytical Chimica Acta.* **2013.** *773,* 9-23.

76) Fagerstam, L.G.; Frostell-Karlsson, A.; Karlsson, R.; Persson, B.; Ronnberg, I. *J. Chromatogr.* **2012.** *597,* 397-410.

77) Schuck, P. Kinetics of ligand binding to receptor immobilized in a polymer matrix, as detected with an evanescent wave biosensor. I. A computer simulation of the influence of mass transport. *Biophys. J.* **1996.** *70,* 1230-1249.

78) Heffler, M.A.; Walters, R.D.; Kugel, J.F. Using Electrophoretic Mobility shift Assays to Measure Equilibrium Dissociation Constants: GAL4-p53 Binding DNA as a Model System. *Biochemistry and Molecular Biology Education.* **2012.** *40,* 383-387.

79) Anderson, B.J.; Larkin, C.; Guja, K.; Schildbach, J.F. using Fluorophore-labeled Oligonucleotides to Measure Affinities of Protein-DNA Interactions. *Methods Enzymol.* **2008.** *450,* 253-272.

80) Altschuler, S.E.; Lewis, K.A.; Wuttke, D.S. Practical strategies for the evaluation of high-affinity protein/nucleic acid interactions. *J. Nucleic Acids Investig.* **2013.** *4,* 19-28.

81) Huang, X.; El-Sayed, M.A. Gold Nanoparticles, optical properties and implementations in cancer diagnosis and photothermal therapy. *Journal of Advanced Research.* **2010,** *1,* 13-28.

82) Daniel, M.C; Astruc, D. Gold Nanoparticles: Assembly, Supramolecular Chemistry, Quantum Size Related Properties and Applications toward Biology, Catalysis and Nanotechnology. *Chem. Rev.* **2004.** *104,* 293-346.

83) Frens G. Controlled nucleation for the regulation of the particle size in monodisperse gold suspensions. *Nat Phys Sci* **1973,** *24*, 20–2.

84) Turkevich J, Stevenson PC, Hillier J. A study of the nucleation and growth processes in the synthesis of colloidal gold. *Disc Farad Soc* **1951**, *11,* 55–75.

85) Turkevich J, Garton G, Stevenson PC. The color of colloidal gold. *J Colloid Sci* **1954**, *9*(Suppl 1):26–35

86) Mie G. A contribution to the optics of turbid media, especially colloidal metallic suspensions. *Ann Phys* **1908**, *25,* 377–445.

87) Kerker M. The scattering of light and other electromagnetic radiation. *New York: Academic Press*; **1969.**

88) Papavassiliou GC. Optical properties of small inorganic and organic metal particles. *Prog Solid State Chem* **1979**, *12,* 185–271.

89) Bohren CF, Huffman DR. Absorption and scattering of light by small particles. *New York: Wiley*; **1983.**

90) Kreibig U, Vollmer M. Optical properties of metal clusters. *Springer*; **1995**.

91) Mie G. A contribution to the optics of turbid media, especially colloidal metallic suspensions. *Ann Phys* **1908**, *25,* 377–445.

92) Frens, G. Controlled Nucleation for the Regulation of the Particle Size in Monodisperse Gold Suspensions. *Nature: Phys. Sci*. **1973,** *241,* 20-22.

93) Hakkinen H. The Gold-Sulfur Interface at the *Nanoscale. Nat. Chem*. **2012,** *4,* 443–55.

94) Pensa E.; Cortes E.; Corthey G.; Carro P.; Vericat C.; Fonticelli M. H.; Benitez G.; Rubert A. A.; Salvarezza R. C. The Chemistry of the Sulfur-Gold Interface: In Search of a Unified Model. *Acc. Chem. Res*. **2012**, *45*, 1183–1192.

95) Fischer, Marcel JE. "Amine coupling through EDC/NHS: a practical approach." *Surface plasmon resonance: methods and protocols* (2010): 55-73

96) Alsager, O.A.; Kumar, S.; Zhu, B.; Travas-Sejdic, J.; McNatty, K.P.; Hodgkiss, J.M. Ultrasensitive colorimetric detection of 17β-estradiol: The effect of shortening DNA aptamer sequences. *Analytical Chemistry.* **2015,** *87,* 4201-4209

97) Guo, Y.; Zhang, Y.; Shao, H.; Wang, Z.; Wang, X.; Jiang, X. Label-Free colorimetric detection of cadmium ions in rice samples using gold nanoparticles. *Analytical Chemistry.* **2014,** *86,* 8530-8534.

98) Chen, L.; Li, J.; Chen, L. Colorimetric Detection of mercurcy species based on functionalized gold nanoparticles. *ACS Appl. Mater. Interfaces.* **2014,** *6,* 15897-15904.

99) Huo,Y.; Qi, L.; Lai, T.; Zhang, J.; Zhang, Z. A sensitive aptasensor for colorimetric detection of adenosine triphosphate based on the protective effect of ATP aptamer complexes on unmodified gold nanoparticles. *Biosensors and Bioelectronics.* **2016,** *78,* 315-320.

100) Lee, B.H.; Nguyen, V.T.; Gu, M.B. Highly sensitive detection of 25-hydroxyvitaminD_3 by using a target-induced displacement of aptamer. *Biosensors and Bioelectronics.* **2017,** *88,* 174-180

101) Gopinath, S.; Lakshmipriya, T.; Awazu, K. Colorimetric detection of controlled assembly and disassembly of aptamers on unmodified gold nanoparticles. *Biosensors and Bioelectronics.* **2014,** *51,* 115-123.

102) Han, X.; Goebl, J.; Lu, Z.; Yin, Y. Role in Salt in the spontaneous assembly of charged gold nanoparticles in ethanol. *Langmuir.* **2011.** *27(9),* 5282-5289